Biological Psychiatry: CNNI

Archival Report

Cognitive Signatures of Depressive and Anhedonic Symptoms and Affective States Using Computational Modeling and Neurocognitive Testing

Nadja R. Ging-Jehli, Manuel Kuhn, Jacob M. Blank, Pranavan Chanthrakumar, David C. Steinberger, Zeyang Yu, Todd M. Herrington, Daniel G. Dillon, Diego A. Pizzagalli, and Michael J. Frank

ABSTRACT

BACKGROUND: Deeper phenotyping may improve our understanding of depression. Because depression is heterogeneous, extracting cognitive signatures associated with severity of depressive symptoms, anhedonia, and affective states is a promising approach.

METHODS: Sequential sampling models decomposed behavior from an adaptive approach-avoidance conflict task into computational parameters quantifying latent cognitive signatures. Fifty unselected participants completed clinical scales and the approach-avoidance conflict task by either approaching or avoiding trials offering monetary rewards and electric shocks.

RESULTS: Decision dynamics were best captured by a sequential sampling model with linear collapsing boundaries varying by net offer values, and with drift rates varying by trial-specific reward and aversion, reflecting net evidence accumulation toward approach or avoidance. Unlike conventional behavioral measures, these computational parameters revealed distinct associations with self-reported symptoms. Specifically, passive avoidance tendencies, indexed by starting point biases, were associated with greater severity of depressive symptoms (R = 0.34, p = .019) and anhedonia (R = 0.49, p = .001). Depressive symptoms were also associated with slower encoding and response execution, indexed by nondecision time (R = 0.37, p = .011). Higher reward sensitivity for offers with negative net values, indexed by drift rates, was linked to more sadness (R = 0.29, p = .042) and lower positive affect (R = −0.33, p = .022). Conversely, higher aversion sensitivity was associated with more tension (R = 0.33, p = .025). Finally, less cautious response patterns, indexed by boundary separation, were linked to more negative affect (R = −0.40, p = .005).

CONCLUSIONS: We demonstrated the utility of multidimensional computational phenotyping, which could be applied to clinical samples to improve characterization and treatment selection.

https://doi.org/10.1016/j.bpsc.2024.02.005

In the United States, the number of adults experiencing depression-related symptoms has quadrupled over the past 4 years (1,2). Probing distinctions between cognitive signatures of depressive and anhedonic symptoms is crucial because this differentiation not only enhances our comprehension of anhedonia but also contributes to a deeper understanding of depression. This is particularly significant because increased anhedonia severity has been linked to worse trajectories in depression (3–5), increased nonresponsiveness to treatments (6–8), and poorer quality of life (9).

Depression and anhedonia have both been associated with multiple affective states (10,11). Characterizing depression, some studies have reported diminished positive affect and excessive negative affect (12,13), while others have found pronounced sadness but intact positive affect (11,14–16). Characterizing anhedonia, some studies have reported flat and blunted responses to pleasurable experiences (17,18), while others have found shorter and/or more variable positive affective responses to pleasurable experiences (19,20). Consequently, this wide range of affective states often manifests in diverse symptom profiles (i.e., phenotypes). Therefore, studies are needed to deconstruct these heterogeneous symptom profiles. For example, distinguishing anhedonia from other symptoms of depression may improve diagnostics and treatment selection, but to date, similarities and differences among cognitive signatures of dimensional depression, anhedonia, and affective states have rarely been explored.

Here, we characterize latent cognitive signatures of depressive symptoms, anhedonia, and affective states by decomposing behavior from (neuro)cognitive tests with

 ISSN: 2451-9022

process-oriented models. This approach is known as multidimensional computational phenotyping (21–31). We focus on symptom severities rather than diagnostic categories, consistent with the conceptualization that mental health conditions generally exist on a continuum rather than as categories (24,31,32). First, we introduce the approach-avoidance conflict (AAC) task as a promising probe for characterizing depressive phenotypes (33–36), highlighting several novel features. Next, we introduce sequential sampling models as powerful process-oriented analytics.

Studying AAC Behavior

In AAC paradigms, participants decide to approach or avoid offers that include both rewarding and aversive features (37). Varying the relative magnitude of these rewarding and aversive features produces offers with different conflict levels. Recent studies found that individuals with major depressive disorder were characterized by distinct neural and behavioral patterns compared to individuals without major depressive disorder (28,38). Specifically, Pedersen *et al.* (28) found that people with major depressive disorder were less sensitive to reward and had lower tendencies to approach offers. However, past studies focused on categorical assessments and did not discriminate between cognitive signatures of dimensional depression, anhedonia, and affective states.

Using AAC paradigms to extract fine-grained signatures of different depression-related constructs requires modification of task specifics to increase their clinical sensitivity. This is because reward and aversion responses in AAC paradigms can be driven by multiple underlying constructs that need to be dissociated. For example, participants' experienced conflict level depends on their so-called marginal rate of substitution between reward and aversion—that is, the willingness to accept an additional unit of aversion for an additional unit of reward. Conversely, participants' sensitivity to changes in either reward or aversion depends on their marginal utilities.[1] Ultimately, reward and aversion responses can also be influenced by asymmetric costs of approach relative to avoidance choices (28,39). All these concepts can affect decision-making processes differently and may involve distinct neural pathways and signaling (40,41).

We implemented a modified AAC task (Figure 1A) to distinguish between the aforementioned concepts. First, offers were composed of reward and aversion by using money and shock as reinforcers. This allowed us to calibrate offers based on individuals' marginal rates of substitution and parametrically manipulate the amount of offered reward and punishment. Second, offers were created on a trial-by-trial basis to separately probe individuals' reward and aversion sensitivities. Third, we distinguished between positive and negative domains because reward and aversion sensitivity may depend on the sign of an offer's net value (42–45). Fourth, we distinguished between instrumental responses that are congruent with Pavlovian approach/avoidance tendencies, making them more automatic than those that are incongruent with these tendencies (Figure 1B) (39,46,47).

[1]The change in subjective value for a marginal increase in reward, keeping constant aversiveness. Marginal utilities reflect the relative change of consumed reward and aversion.

Sequential Sampling Modeling

We focused on a process-oriented account by fitting sequential sampling models (SSMs) to behavioral data from the AAC task (24,48). Conventional performance measures and alternative cognitive models (e.g., signal detection theory models) focus either on response times (RTs) or response frequencies (24). Conversely, SSMs simultaneously account for the entire RT distribution and the relative frequency of each response option, thus providing richer analytical information (49,50). SSMs simulate behavior with processes that sequentially accumulate information up to a decision threshold (49,51–53). This allows the decomposition of behavior into distinct, quantifiable mental components with established psychological interpretations.

The diffusion decision model (54) is a prominent SSM (Figure 2A) with 4 main parameters (28,50). Specifically, drift rate (v) reflects the quality of evidence accumulation. In our context, higher drift rates indicate easier decisions, such that evidence accumulates more rapidly, resulting in faster RTs and more frequent approach choices. Boundary separation (a) reflects the required amount of evidence for reaching decisions. Larger boundary separations yield more consistent choices (i.e., less variability in choosing different actions for offers with similar levels of evidence), resulting in slower (and more skewed) RTs. Starting points (z) indicate initial response biases (e.g., due to asymmetric costs of stimulus-response mapping). In our context, larger starting points indicate greater biases toward approach choices, which leads to large changes in the tail and leading edge of the RT distributions. Finally, longer nondecision time (T_{er}) indicates longer perceptual encoding and response execution times that occur outside the decision process, shifting the entire RT distribution but without affecting its shape.

Only a few studies have examined AAC behavior with computational models, and most of them did not use SSMs (55–59). The few studies that applied SSMs only used the classic diffusion decision model and focused on categorical assessments of depression (28,34,60,61). However, different SSMs assume distinct dynamics in decision-making processes that can lead to different behavioral predictions (49,52,62,63). For example, collapsing boundaries (Figure 2B) are used to model the declining need for additional evidence as time passes (e.g., when participants become increasingly impatient or when externally or internally imposed response deadlines are imposed) (64–67). Therefore, we tested different models to find the one that accounted best for the behavioral pattern (24,68).

METHODS AND MATERIALS

Participants

Fifty adults were recruited through the Harvard Psychology Community Study Pool. Inclusion was restricted to adults between ages 18 and 45 years who were fluent in English and not color blind; note that this study pool does not consist solely of Harvard students. Participants were not preselected

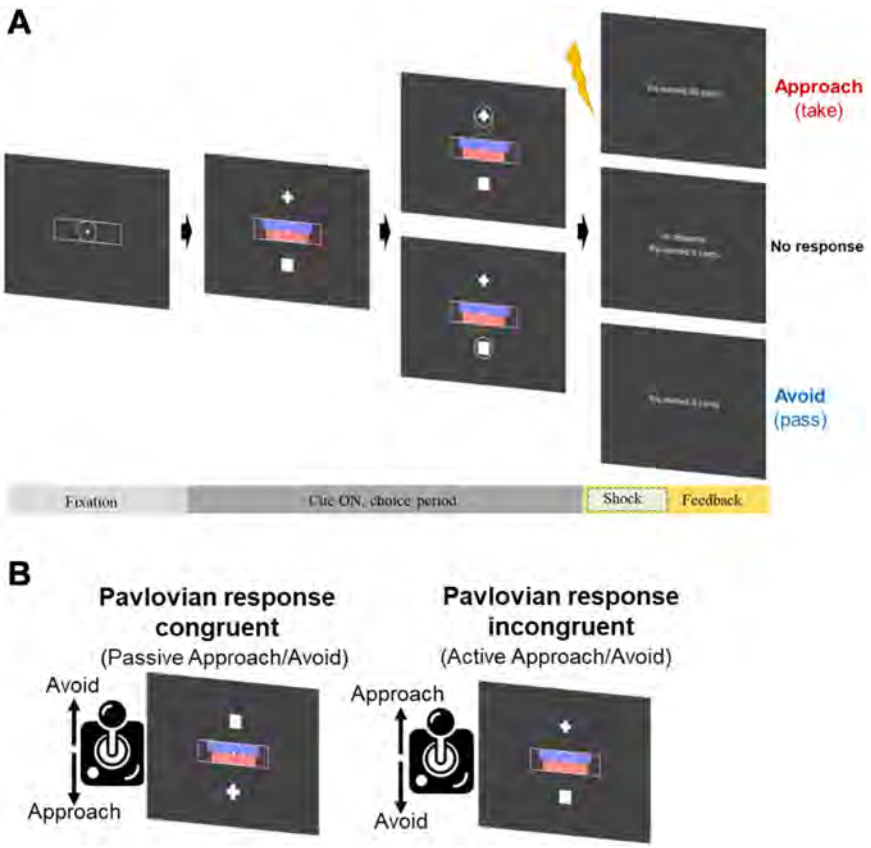

Figure 1. Approach-avoidance conflict task. **(A)** Participants decided to approach or avoid offers with monetary reward (magnitude represented by blue bars) and electrical shock (magnitude represented by red bars). **(B)** Trials were counterbalanced including either Pavlovian response-congruent trials or Pavlovian response-incongruent trials.

based on clinical measures or evaluated using clinical interviews. They received $22.50 for performing the AAC task and completing the clinical questionnaires and a performance-based bonus (maximal $27.10). For process-oriented computational analyses, all 50 datasets were used, whereas 2 participants were omitted from questionnaire-based analyses because they did not complete the self-report assessments.

AAC Paradigm

A total of 105 offers were presented one at a time. Each offer was composed of a monetary reward component and an aversive (electrical shock) component displayed by horizontal bars (Figure 1). After a fixation period, response symbols (i.e., a plus sign represented approach choices, while a square represented avoidance choices) were simultaneously presented with the offer. Offers were dynamically created on a trial-by-trial basis for each participant. See the Supplement for additional details.

Beck Depression Inventory-II

The Beck Depression Inventory-II (69) assesses the severity of depressive symptoms (70,71). Participants rate each symptom during the past 2 weeks on a scale from 0 (not feeling or experiencing the symptom) to 3 (feeling or experiencing the symptom to an extreme extent). Raw scores range from 0 to 63, with scores below 13 indicating minimal to no depression severity. Scores from 14 to 19, 20 to 28, and >29 indicate mild, moderate, and severe depression severity, respectively.

Snaith-Hamilton Pleasure Scale

The Snaith-Hamilton Pleasure Scale (72) assesses hedonic capacity (41,73,74) and consists of 14 statements that assess an individual's capacity to experience pleasure. Participants indicate their agreement with each statement, considering the previous few days, on a scale from 1 (definitely agree) to 4 (definitely disagree). Total scores range from 14 to 56, with higher scores representing more anhedonia.

Positive and Negative Affect Schedule

The Positive and Negative Affect Schedule (PANAS) (75) assesses positive affect and negative affect. Respondents indicate how strongly they identify with 20 descriptions on a scale of 1 (very slightly or not at all) to 5 (extremely) based on their mood during the past 2 weeks (75). The PANAS yields 2 scores (PANAS–positive affect and PANAS–negative affect) ranging from 10 to 50, with higher scores indicating greater levels of positive or negative affect.

Visual Analog Mood Scale

The Visual Analog Mood Scale (76) assesses current mood states. Participants view horizontal lines ranging from 0 to 100, each corresponding to a bipolar mood spectrum: happy-sad,

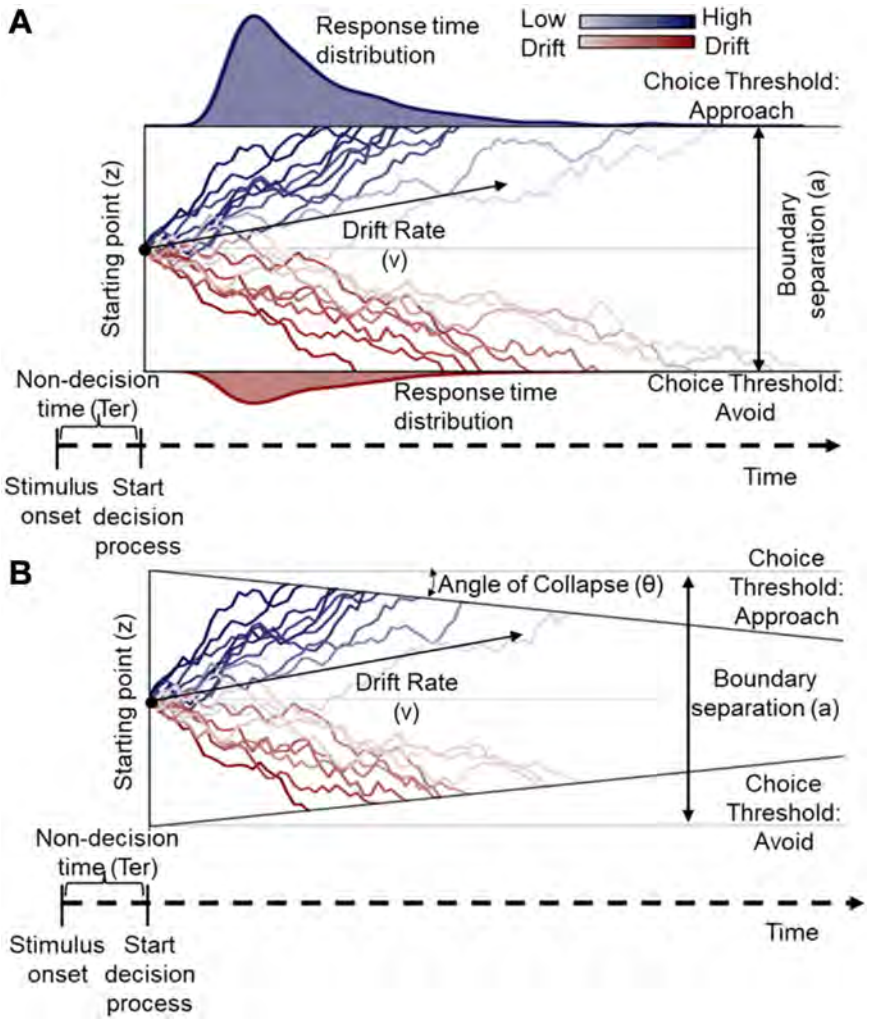

Figure 2. Computational account of behavior in the approach-avoidance conflict task decomposed decision processes into distinct and quantifiable latent cognitive components. **(A)** The diffusion decision model [Ratcliff (54)] simulates decisions by noisy evidence processes that evolve over time toward one of the 2 boundaries that represent the 2 response options. The set of model parameters (e.g., T_{er}, z, a, v) reproduces behavior, whereby each parameter quantifies a distinct cognitive signature of the decision dynamics. **(B)** An alternative sequential sampling model with linear collapsing decision boundaries that presumes different decision dynamics than the diffusion decision model.

tense-relaxed, and friendly-hostile. Participants choose a point on each line that best characterizes their current mood. We converted the scores on each scale such that higher scores indicated more negative affect.

Mood and Anxiety Symptom Questionnaire

The Mood and Anxiety Symptom Questionnaire (77) assesses symptoms related to anxiety and depression. Participants rate the presence of 62 symptoms during the past week on a scale from 1 (very slightly or not at all) to 5 (extremely). We used the anxiety-related subscores—general distress: anxiety and anxious arousal—to account for anxiety-related symptoms.

Cognitive and Behavioral Avoidance Scale

The Cognitive and Behavioral Avoidance Scale (78) assesses avoidance behavior associated with anxiety and depression. Thirty-one items describe different avoidant behaviors that participants rate on a scale from 1 (not at all) to 5 (extremely). A higher score indicates more avoidance tendencies.

Questionnaire Assessment

All scales had excellent internal reliability (Cronbach's alpha ranging from 0.82 to 0.94) (see the Supplement and Figure S1).

Analytics

We fit different versions of SSMs to single-trial RTs and choices within a Bayesian hierarchical framework using the open-source toolbox HDDM (64,65,79) (see the Supplement). Then, we selected the best model in terms of both deviance information criterion and posterior predictive checks. Because offers (i.e., presented reward, aversiveness, conflict) varied on each trial, model parameters specified by these stimulus attributes also varied on a trial-by-trial basis. We provide model comparison in the Supplement and focus on clinical relationships with the best-fitting model. The Supplement also provides parameter recovery assessments by generating simulated data (using the participants' offers and the estimated model parameters as inputs) and then determining whether the fitted parameters were recovered. We examined posterior

distributions of estimated coefficients to assess their significance in simultaneously predicting RTs and choices on a trial-by-trial basis. For brevity, we report point estimates (posterior means) and 95% CIs for all covariates in the Supplement.

Computational Phenotyping

To explore links between symptoms and computational model parameters, we first conducted correlational analyses between the parameters of the best-fitting model and raw questionnaire scores. We examined the linearity of correlations with scatterplots (Supplement). After identifying statistically significant associations, we assessed the clinical relevance of these associations with multivariate regression models. Specifically, the questionnaire scores served as dependent variables, while the model parameters served as predictors. Covariates were *z* scored before entering the regression models. We compared model performance with *F* test analyses. We provide additional sensitivity analyses in Tables S8 and S9. To establish the benefits of SSM parameters over conventional performance measures, we estimated multivariate regression models with mean RTs and choice frequencies as predictors (with severity scores as dependent variables).

RESULTS

Our sample (n = 50) included 35 women (mean age = 29 years, SD = 7 years) with a broad range of symptom severity related to depression and anhedonia (but low levels of anxiety) (see Table S1 and Figure S2).

Relative Frequency and Speed of Decisions Depended on Domain Type

Figure 3 simultaneously presents choice frequencies and RT quantiles. Offers with positive net values (reward minus aversiveness) comprise the positive domain, while those with negative net values comprise the negative domain. Across both domains, the frequency of approach decisions increased as the offers' net values increased. This pattern is consistent with an evidence accumulation model wherein the strength of net evidence accumulation (drift rate) for approach is proportional to the difference between reward and aversion.

Models With Linear Collapsing Boundaries Performed Best

The SSM with linear collapsing boundaries outperformed other SSM versions in terms of both the deviance information criterion and posterior predictive checks (Tables S2, S3; Figures S3, S4). Overall, simulations showed good parameter recovery, particularly for the parameters that are included in the main analysis presented below (Figure S5). The recovery of drift rates for the positive domain was poorer than for the negative domain, leading to lower power to detect effects in the positive domain. Figure S6 shows that this was due to the trial-by-trial creation of offers, which led to a higher sampling of reward-aversion combinations for the negative domain (due to less consistent choices of approach relative to avoidance) than the positive domain. Therefore, we do not overly interpret the difference between positive and negative domains.

The best-fitting model (Figure 3B; Figure S7) included linear boundary collapses that varied by conflict (defined as the absolute difference between reward and aversion). Drift rates toward approach varied by reward, aversion, and domain type. Higher conflict was associated with decreased boundary separation (a: mean posterior point estimate $\beta = -0.035$, SD = 0.017) and slower collapsing rates (θ: $\beta = -0.031$, SD = 0.012). Statistics for posterior distributions are presented in Table S4, and correlations between parameters are provided in Figure S8.

Multidimensional Computational Phenotyping

The severity of depression and anhedonia were moderately correlated ($R = 0.51$, $p \leq .001$). Correlational analyses between best-fitting model parameters and questionnaire scores identified cognitive signatures of depression severity, anhedonia, and affective states (Figure 4A). Figure 4B, C shows the linear associations for 2 parameters (also see Figures S9 and S10).

Distinguishing Between Depressive and Anhedonic Symptoms

Greater depression severity was associated with weaker approach biases on a Pavlovian congruent (passive avoidance) trial (zPB_c: $R = -0.34$, $p = .019$) (Figure 4A), accounting for asymmetric effects in the RT distributions of avoidance versus approach choices. Moreover, greater depression severity was associated with longer nondecision times (T_{er}: $R = 0.37$, $p = .011$) (Figure 4A), accounting for right-shifted RT distributions of both choice types.[2]

A multivariate regression model with depression severity as the dependent variable and computational parameters (T_{er}, zPB_c) as independent variables showed that depression severity was related to both nondecision time (T_{er}: coefficient $\beta = 0.319$, SD = 0.134, $p = .022$) and passive avoidance tendencies (zPB_c: $\beta = -0.286$, SD = 0.134, $p = .038$), adjusted $R^2 = 0.179$. Subsequent F test analyses illustrated that this multivariate model (M1), which included both parameters as main effects, outperformed alternative, univariate models (Table S5).

Dissecting Reward and Aversion Sensitivity and Their Associations With Affective States

Increased reward sensitivity in the negative domain (Figure 4A: $v_{reward,neg}$) was associated with lower positive affect ($p = .022$) and more sadness ($p = .042$). This means that for adults who endorsed lower positive affect and more sadness, marginal reward increases were less effective in switching choices from avoidance to approach when offers had negative net values.

While positive affect and sadness were inversely related to reward sensitivity in the negative domain, more tension was associated with increased aversion sensitivity in that domain ($v_{averse,neg}$: $p = .025$) (Figure 4A). More tension was also associated with faster decision boundary collapses as conflict increased ($\theta_{conflict}$: $p = .049$) (Figure 4A). However, the

[2]Follow-up analyses showed a strong positive association between depression severity and severity of universal avoidance behavior ($R = 0.81$, $p < .001$) as measured by the total score on the Cognitive and Behavioral Avoidance Scale (see Methods and Materials). Cognitive and Behavioral Avoidance Scale–related avoidance severity was also solely associated with longer nondecision time ($R = 0.31$, $p = .031$).

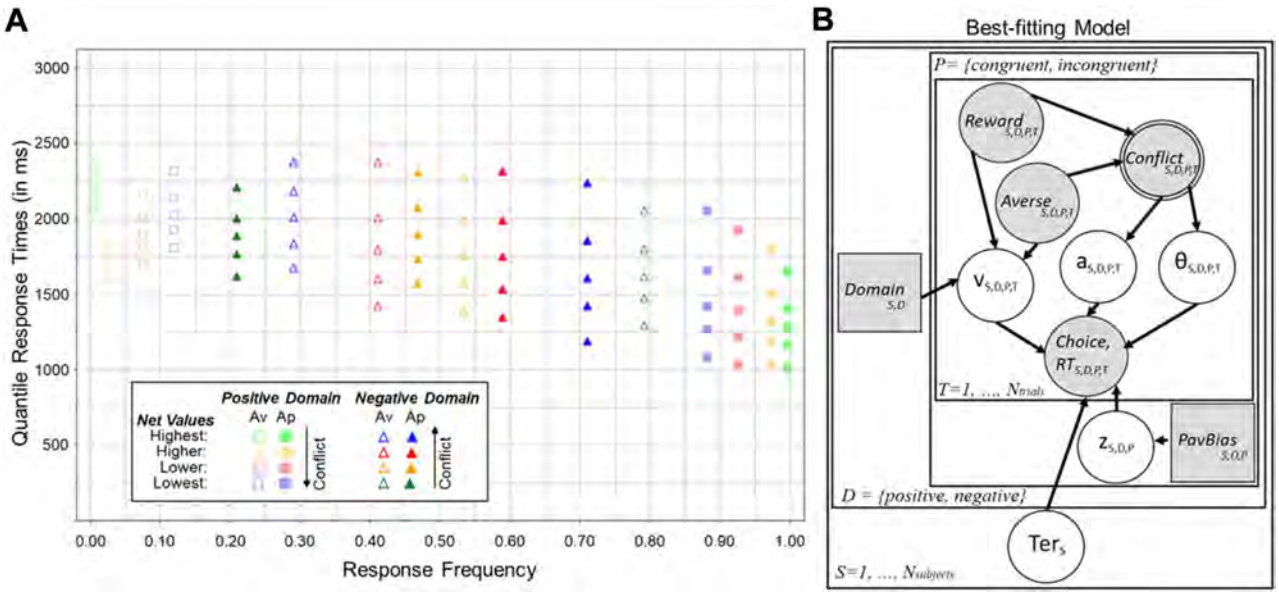

Figure 3. Reducing conflict increased the frequency of approaches and enhanced the consistency of decisions. **(A)** Quantile-probability plot for offers that were equally binned (for each domain separately) into 4 conditions (highest, higher, lower, lowest) based on their net values. Note that offers were binned for illustration purposes only. The x-axis represents choice frequency of approach (filled symbols) and avoidance (unfilled symbols). Vertical columns represent the quantile response times, referring to the 0.1, 0.3, 0.5 (median), 0.7, and 0.9 quantiles when moving from bottom to top. As conflict decreased, approaches occurred more frequently, and their speed became less dispersed (more consistent). The 2 domains also induced distinct effects on the relative speed of approach vs. avoidance decisions. **(B)** Graphical representation of the best-fitting model that included linear collapsing boundaries. Shaded nodes represent observed variables, and nonshaded nodes represent estimated parameters. Circles represent continuous variables; squares represent discrete variables. Conflict refers to the absolute difference between reward and aversion and is therefore computed and double bordered. Drift rates varied by offers and their domains, while boundary separation and their linear collapses varied by conflict. Starting points varied by active/passive approach tendencies. θ, angle of linear collapse; *a*, boundary separation; Ap, approach; Av, avoidance; D, domain; P, Pavlovian congruency; PavBias, Pavlovian bias; RT, response time; S, subjects; T, trials; T_{er}, nondecision time; *v*, drift rate; *z*, starting points.

multivariate model (M1) with tension as the dependent variable and both parameters ($v_{averse,neg}$, $\theta_{conflict}$) as main effects did not perform better than a univariate model (M2) with only $v_{averse,neg}$ as a covariate (Table S5). Therefore, tension seemed to be predominantly associated with increased aversion sensitivity in the negative domain.

Cognitive Signatures of Negative Affect

More negative affect was associated with decreased boundary separation (*a*: $p = .005$) (Figure 4A), leading to less consistent response patterns for offers close to the border of the positive and negative domain. Additionally, more negative affect was associated with more active approach tendencies (zPB_i: $p = .023$) (Figure 4A). Multivariate regression models revealed an association between the magnitude of negative affect and a main effect of boundary separation (*a*: $\beta = -0.366$, SD = 0.128, $p = .007$) and its interaction with active approach tendencies (*a*-by-zPB_i interaction: $\beta = -0.335$, SD = 0.131, $p = .014$), but the main effect of active approach was no longer significant (zPB_i: $\beta = 0.137$, SD = 0.135, $p = .318$), adjusted $R^2 = 0.272$. Therefore, participants with less cautious response patterns exhibited more negative affect, even more so if they also demonstrated active approach tendencies. Subsequent *F* test analyses showed that the multivariate model (M1) that included both model parameters and their interaction outperformed alternative multivariate and univariate models (Table S5).

Computational Phenotyping Versus Summary Statistics

Next, we evaluated whether computational parameters were better predictors of clinically relevant constructs than conventional performance measures. Figure 5 shows the estimated coefficients from multivariate regression models with clinical constructs (1 per subplot) as dependent variables. Model A included conventional performance measures as covariates, while models B and C included computational parameters as covariates. As marked by the asterisks (indicating statistical significance) in Figure 5, only the computational parameters were related to clinical constructs (except for the case where mean RT was related to negative affect, shown in Figure 5C). Additional statistics are provided in Tables S6 and S7.

DISCUSSION

In an unselected community sample with varying symptoms, we probed cognitive signatures related to depressive symptom severity, anhedonia, and affective states in an AAC task with computational modeling. The SSM that accounted best for the decision dynamics included linear collapsing boundaries that varied by conflict, starting points that varied by response modes, and domain-specific drift rates that distinguished between reward and aversion sensitivity. Critically, this process-oriented account deconstructed behavior into separate and

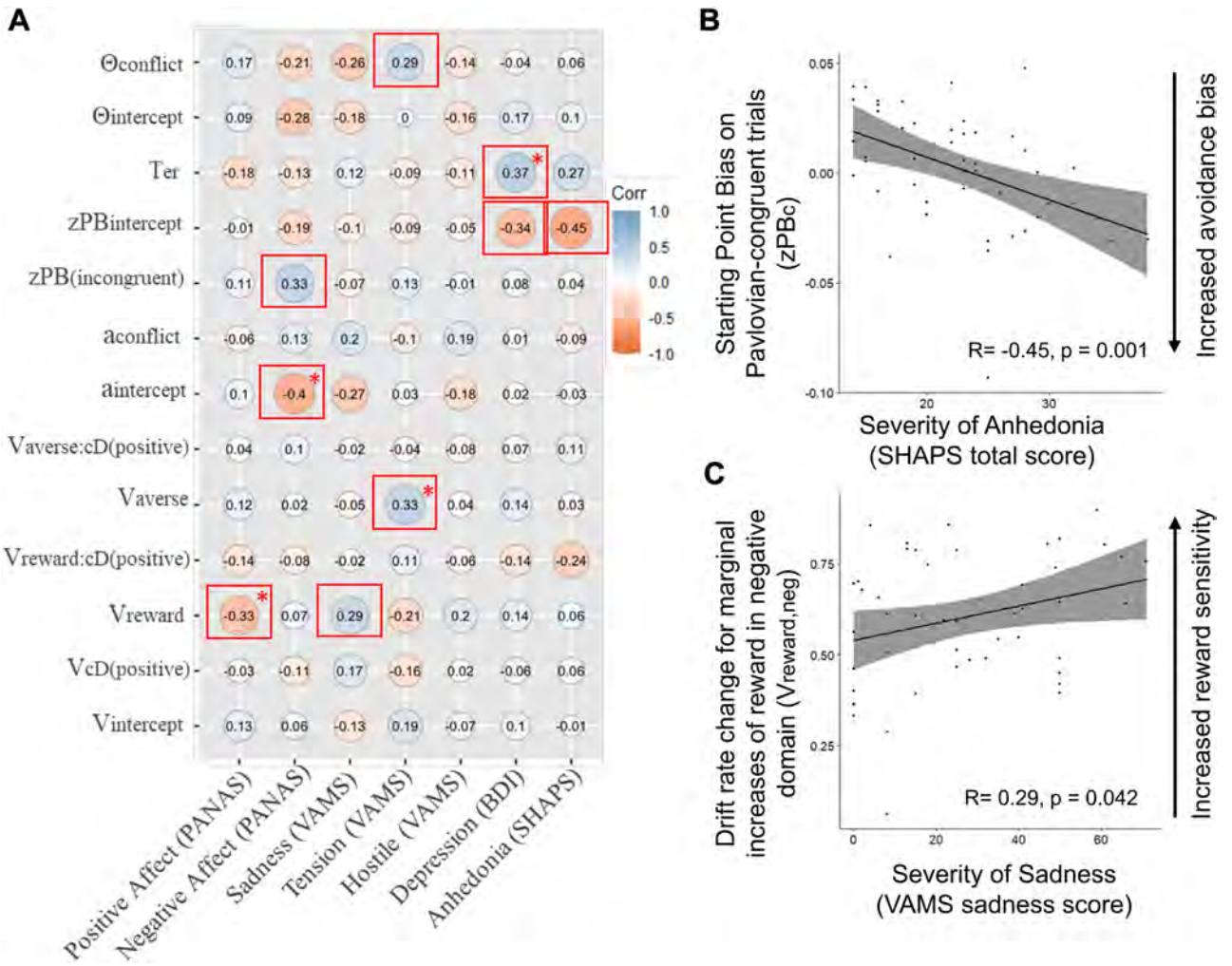

Figure 4. Different cognitive characteristics of depressive and anhedonic symptoms and affective states. **(A)** Depressive symptoms, anhedonia, and affective states were correlated with distinct cognitive signatures as indexed by varying model parameters (a refers to boundary separation, cD refers to the domains [positive, negative], PB refers to the Pavlovian response incongruent/congruent trials, Ter refers to nondecision time, θ refers to angle of linear collapse, v refers to drift rate, and z refers to starting points. Significant (p values $<$ .05 and unadjusted for multiple comparisons) correlations are surrounded by red boxes. For correlation pairs that showed a moderate to strong correlation strength ($R \geq 0.30$), we also estimated p values adjusted using false discovery rate correction. The correlations that showed an adjusted p value $<$ .05 are also marked by an asterisk. Figure S9 shows the complete matrix including significant and nonsignificant correlations. **(B)** Linear association between anhedonia and starting point bias for Pavlovian-congruent trials. Black dots indicate data. Means (solid lines) and corresponding 95% CIs are shown as shaded intervals. **(C)** Linear association between sadness and drift rate for marginal reward changes in the negative domain. BDI, Beck Depression Inventory; Corr, correlation; PANAS, Positive and Negative Affect Schedule; SHAPS, Snaith-Hamilton Pleasure Scale; VAMS, Visual Analog Mood Scale.

quantifiable components (cognitive signatures) that were associated with distinct clinical constructs. We also demonstrated the utility of computational phenotyping over conventional performance measures by showing that, with one exception, SSM parameters were more predictive of symptom scores.

Our adaptive AAC task, together with computational modeling, allowed us to separate behavioral effects due to conflict and impatience (indexed by boundary separation and boundary collapses), response biases (indexed by starting points), and reward and aversion sensitivity (indexed by drift rates). In previous studies, estimated reward and aversion sensitivity could have been influenced by individual differences in preferences, marginal rates of substitutions, and/or differences in relative potency, timing, and duration of reward and aversion (41,80).

Anhedonia and depressive symptoms were both associated with more passive avoidance tendencies. However, greater depressive symptoms were uniquely associated with longer nondecision times. At first, this may seem to contradict findings from previous studies that found depression characteristics to manifest in drift rates and starting point biases (81,82). However, these studies focused on categorical assessments of depression and used tasks (e.g., perceptual discrimination tasks) that are meant to tap into other cognitive constructs. This is important to consider because task specifics determine the precise interpretations of model parameters (24).

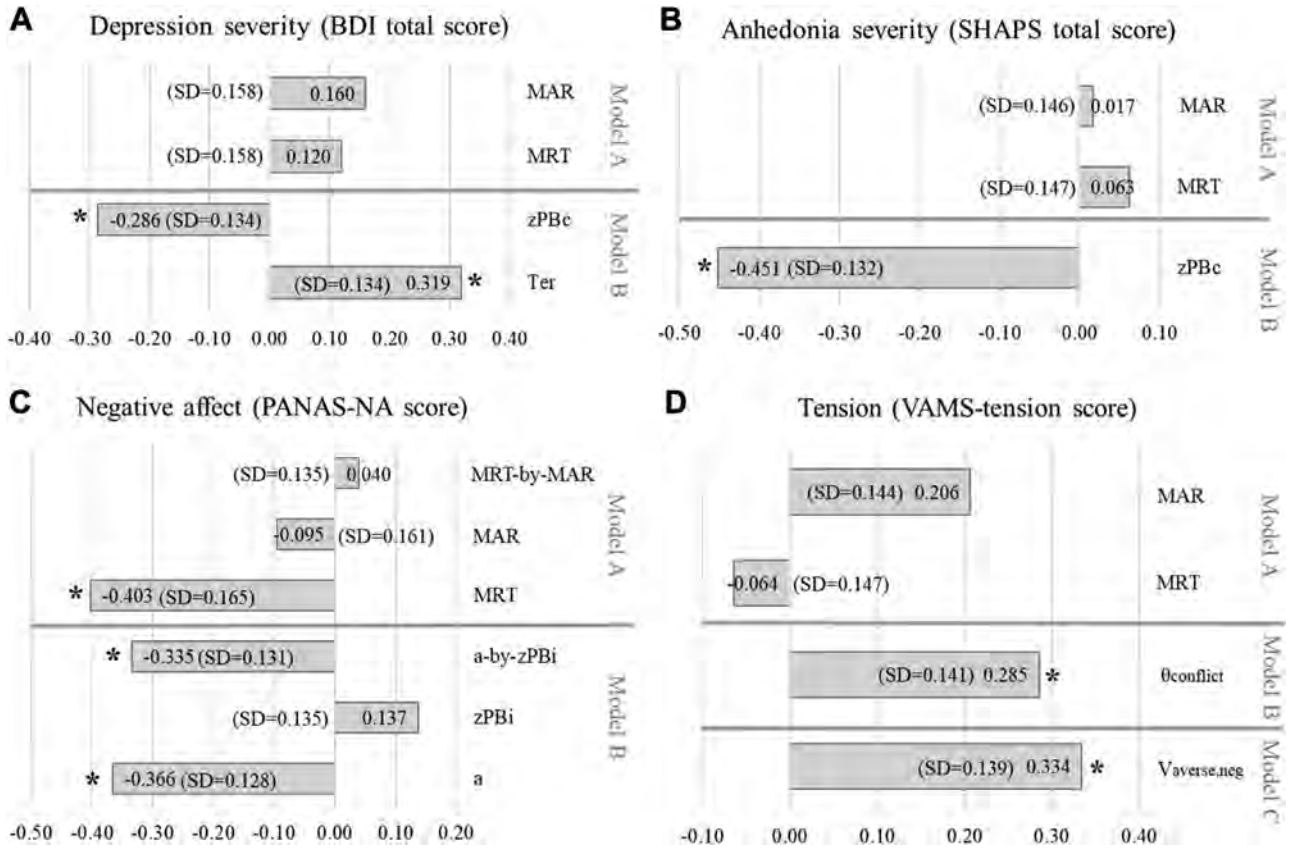

Figure 5. Computational parameters were correlated with symptom scores, whereas summary statistics (mean frequency rates and mean response times) were not. Shown are regression coefficients (means and SDs) of different models specified subsequently. Asterisks indicate significant regressors ($p < .05$). Regression outputs are provided in Tables S5 and S6. **(A)** Models with depression severity as the dependent variable. Model A included main effects of mean approach frequency (MAR) and mean response time (MRT) as covariates. Model B included main effects of nondecision time (T_{er}) and starting point bias on Pavlovian-incongruent trials ($zBias_i$) as covariates. **(B)** Models with anhedonia severity as the dependent variable. Model A included main effects of MAR and MRT as covariates. Model B included the main effect of starting point bias on Pavlovian-congruent trials ($zBias_c$) as covariate. **(C)** Models with negative affect (NA) as the dependent variable. Model A included main effects of MAR and MRT as covariates. Model B included main effects of boundary separation (for average conflict trials) and starting point bias on Pavlovian-incongruent trials ($zBias_i$) as well as their interaction as covariates. **(D)** Models with tension severity as the dependent variable. Model A included main effects of MAR and MRT as covariates. Model B included the rate of the boundary collapse on trials with higher conflict than average ($\theta_{conflict}$) as covariate. Model C included aversion sensitivity (indicated by drift rate) in the negative domain ($v_{averse,neg}$) as covariate. BDI, Beck Depression Inventory; PANAS, Positive and Negative Affect Schedule; SHAPS, Snaith-Hamilton Pleasure Scale; VAMS, Visual Analog Mood Scale.

Therefore, the specifics of our task (i.e., forming a representation of reward relative to aversion by extracting the relative size of horizontal bars without providing an explicit reference point) might have made it more sensitive to detecting clinical differences in early-stage components of decision processes.

Clinical measures of depression and anhedonia comprise heterogeneous symptom profiles. Therefore, it is not surprising that measures of more specific affective states show stronger associations with reward and aversion sensitivities. Our findings highlight that distinct latent cognitive signatures (quantified and estimated by the computational model parameters) can help to define different phenotypes (e.g., decreased positive affect in a subgroup of people with depression) (83,84).

Higher positive affect was associated with decreased reward sensitivity (in the negative domain). This is consistent with previous research suggesting that positive affect can lead to optimistic biases in negative contexts and therefore less sensitive responses to changes in reward (85). Moreover, we found that more sadness was associated with increased reward sensitivity in the negative domain. Because depression can lead to reduced positive affect (10,83) and/or increased sadness (17), our study shows how these affective states are linked to different decision-making biases, in addition to those influenced by the severity of depression itself.

Higher negative affect was associated with both elevated approach under active response mode and less consistent choice patterns for offers with average conflict levels. It is intriguing that positive and negative affect as measured by the PANAS (75) mapped onto different model parameters. However, this finding is consistent with the notion that positive and negative affect are divergent concepts rather than 2 sides of the same coin (86–89).

Tension has been proposed as one of the defining components of mood (90). We found more tension to be associated

with increased urgency signals (more impatience) as conflict increased (i.e., faster collapsing decision boundaries). This is consistent with previous research that associated relaxation (the opposite end of the Visual Analog Mood Scale spectrum from tense to relaxed) with low urgency signals (90).

Limitations and Outlook

We focused on 2 widely used measures to assess severity of depression [Beck Depression Inventory-II (69)] and anhedonia [Snaith-Hamilton Pleasure Scale (72)] and a few affect and mood measures known to be modulated by depression. More research is needed to link cognitive processes to other clinical measures that are sensitive to various aspects of depression and anhedonia. Specifically, future studies should target larger sample sizes and sample across the entire severity spectrum, as well as consider categorical assessments, comorbid diagnoses, and sex differences to further increase the generalizability of our results (74,77). While our sample showed only marginal variability in anxiety severity, future studies that apply multidimensional computational phenotyping are needed to dissociate anxiety-related and depression-related cognitive signatures as well as possible distinct neurobiological mechanisms. Finally, task design and model configurations should be co-developed to guarantee optimal parameter recovery. We emphasize that some model parameters showed better recovery in supplementary recovery analyses. While we focused our interpretation on the model parameters that showed robust recovery, other relationships may exist between parameters and scores that we did not have sufficient power to detect (e.g., measurement errors) due to a restricted range of symptoms.

The main purpose of this study was to explore associations between model parameters and symptom severity of depression, anhedonia, and affective states using an adaptive AAC task and computational modeling. These associations need to be tested more rigorously in future studies that also include more representative samples as detailed above.

Understanding how different affective states map onto distinct cognitive biases is important because it may help to define phenotypes of depression as well as new mechanisms that can be targeted in clinical interventions (26,74,91–93). Identifying how different affective states manifest in behavior is also critical for differential diagnostics and for assessing other co-occurring disorders (e.g., attention-deficit/hyperactivity disorder) that are often also characterized by mood disturbances but due to distinct hypothesized mechanisms (26,31,94,95).

ACKNOWLEDGMENTS AND DISCLOSURES

This work was partially supported by the National Institute of Mental Health (Grant Nos. P50MH119467 [to DAP and MJF]; P50MH106435-06A1 [to MJF]; T32MH126388-01 [to MJF and NRG-J]; R01MH084840 and R01MH115905-01 [to MJF]; R01MH111676 [to DGD]; R01MH108602, R37MH068376, and R01MH101521 [to DAP]; and K23NS099380 [to TMH]). The funders had no role in study design, data collection, or analysis. The content is solely the responsibility of the authors and does not necessarily represent the official views of the National Institutes of Health. This work was conducted using computational resources and services at the Center for Computation and Visualization, Brown University, which is supported by the National Institutes of Health (Grant No. S10OD025181).

We thank the Nock Lab in the Department of Psychology at Harvard University for providing the facilities to conduct this study.

NRG-J has received research funding from the Swiss National Science Foundation and the National Institute of Mental Health. She also co-founded BGBehavior LLC. TMH has received consulting fees from Medtronic, Inc.; he has received stock options from MarvelBiome. MJF has received consulting fees from F. Hoffman La Roche Pharmaceuticals for activities unrelated to this project. Over the past 3 years, DAP has received consulting fees from Boehringer Ingelheim, Compass Pathways, Engrail Therapeutics, Karla Therapeutics, Neumora Therapeutics (formerly BlackThorn Therapeutics), Neurocrine Biosciences, Neuroscience Software, Otsuka, Sama Therapeutics, Sage Therapeutics, Sunovion, and Takeda; honoraria from the American Psychological Association, Psychonomic Society, and Springer (for editorial work) and from Alkermes; research funding from the Brain and Behavior Research Foundation, Dana Foundation, Wellcome Leap, Millennium Pharmaceuticals, and the National Institute of Mental Health; and stock options from Compass Pathways, Engrail Therapeutics, Neumora Therapeutics, and Neuroscience Software. No funding from these entities was used to support the current work, and all views expressed are solely those of the authors. All other authors report no biomedical financial interests or potential conflicts of interest.

ARTICLE INFORMATION

From the Carney Institute for Brain Science, Department of Cognitive, Linguistic, & Psychological Sciences, Brown University, Providence, Rhode Island (NRG-J, PC, MJF); Center for Depression, Anxiety and Stress Research, McLean Hospital, Belmont, Massachusetts (MK, JMB, DCS, DGD, DAP); Department of Psychiatry, Harvard Medical School, Boston, Massachusetts (MK, DGD, DAP); Warren Alpert Medical School of Brown University, Providence, Rhode Island (PC); and Department of Neurology, Massachusetts General Hospital, Harvard Medical School, Boston, Massachusetts (ZY, TMH).

NRG-J and MK are joint first authors.

DAP and MJF are joint senior authors.

Address correspondence to Nadja R. Ging-Jehli, Ph.D., at nadja@gingjehli.com.

Received Aug 9, 2023; revised Feb 3, 2024; accepted Feb 9, 2024.

Supplementary material cited in this article is available online at https://doi.org/10.1016/j.bpsc.2024.02.005.

REFERENCES

1. Panchal N, Kamal R, Cox C, Garfield R (2021): The implications of COVID-19 for mental health and substance use. Omeka Available at: https://is101fall2021.web.illinois.edu/items/show/467. Accessed April 20, 2023.
2. Reinert M, Fritze D, Nguyen T (2022): The State of Mental Health in America 2023. Alexandria, VA: Mental Health America.
3. McMakin DL, Olino TM, Porta G, Dietz LJ, Emslie G, Clarke G, *et al.* (2012): Anhedonia predicts poorer recovery among youth with selective serotonin reuptake inhibitor treatment–resistant depression. J Am Acad Child Adolesc Psychiatry 51:404–411.
4. Moos RH, Cronkite RC (1999): Symptom-based predictors of a 10-year chronic course of treated depression. J Nerv Ment Dis 187:360–368.
5. Wardenaar KJ, Giltay EJ, van Veen T, Zitman FG, Penninx BWJH (2012): Symptom dimensions as predictors of the two-year course of depressive and anxiety disorders. J Affect Disord 136:1198–1203.
6. Spijker J, Bijl RV, de Graaf R, Nolen WA (2001): Determinants of poor 1-year outcome of DSM-III-R major depression in the general population: Results of the Netherlands Mental Health Survey and Incidence Study (NEMESIS). Acta Psychiatr Scand 103:122–130.
7. Uher R, Perlis RH, Henigsberg N, Zobel A, Rietschel M, Mors O, *et al.* (2012): Depression symptom dimensions as predictors of antidepressant treatment outcome: Replicable evidence for interest-activity symptoms. Psychol Med 42:967–980.
8. Wang S, Leri F, Rizvi SJ (2021): Anhedonia as a central factor in depression: Neural mechanisms revealed from preclinical to clinical evidence. Prog Neuropsychopharmacol Biol Psychiatry 110:110289.

9. Whitton AE, Kumar P, Treadway MT, Rutherford AV, Ironside ML, Foti D, *et al.* (2023): Distinct profiles of anhedonia and reward processing and their prospective associations with quality of life among individuals with mood disorders. Mol Psychiatry. [published online Jul 4].
10. Flores-Kanter PE, Garrido LE, Moretti LS, Medrano LA (2021): A modern network approach to revisiting the Positive and Negative Affective Schedule (PANAS) construct validity. J Clin Psychol 77:2370–2404.
11. van Roekel E, Bennik EC, Bastiaansen JA, Verhagen M, Ormel J, Engels RCME, Oldehinkel AJ (2016): Depressive symptoms and the experience of pleasure in daily life: An exploration of associations in early and late adolescence. J Abnorm Child Psychol 44:999–1009.
12. Bylsma LM, Taylor-Clift A, Rottenberg J (2011): Emotional reactivity to daily events in major and minor depression. J Abnorm Psychol 120:155–167.
13. Clark LA, Watson D, Mineka S (1994): Temperament, personality, and the mood and anxiety disorders. J Abnorm Psychol 103:103–116.
14. Peeters F, Nicolson NA, Berkhof J, Delespaul P, deVries M (2003): Effects of daily events on mood states in major depressive disorder. J Abnorm Psychol 112:203–211.
15. Power MJ, Tarsia M (2007): Basic and complex emotions in depression and anxiety. Clin Psychol Psychother 14:19–31.
16. Werner-Seidler A, Banks R, Dunn BD, Moulds ML (2013): An investigation of the relationship between positive affect regulation and depression. Behav Res Ther 51:46–56.
17. Husain M, Roiser JP (2018): Neuroscience of apathy and anhedonia: A transdiagnostic approach. Nat Rev Neurosci 19:470–484.
18. Saxena A, Luking KR, Barch DM, Pagliaccio D (2017): Individual differences in hedonic capacity, depressed mood, and affective states predict emotional reactivity. Motiv Emot 41:419–429.
19. Heininga VE, Van Roekel E, Ahles JJ, Oldehinkel AJ, Mezulis AH (2017): Positive affective functioning in anhedonic individuals' daily life: Anything but flat and blunted. J Affect Disord 218:437–445.
20. Heininga VE, Dejonckheere E, Houben M, Obbels J, Sienaert P, Leroy B, *et al.* (2019): The dynamical signature of anhedonia in major depressive disorder: Positive emotion dynamics, reactivity, and recovery. BMC Psychiatry 19:59.
21. Abramovitch A, Short T, Schweiger A (2021): The C Factor: Cognitive dysfunction as a transdiagnostic dimension in psychopathology. Clin Psychol Rev 86:102007.
22. East-Richard C R, Mercier A, Nadeau D, Cellard C (2020): Transdiagnostic neurocognitive deficits in psychiatry: A review of meta-analyses. Canadian Psychology/Psychologie canadienne 61:190–214.
23. Geana A, Barch DM, Gold JM, Carter CS, MacDonald AW, Ragland JD, *et al.* (2022): Using computational modeling to capture schizophrenia-specific reinforcement learning differences and their implications on patient classification. Biol Psychiatry Cogn Neurosci Neuroimaging 7:1035–1046.
24. Ging-Jehli NR, Ratcliff R, Arnold LE (2021): Improving neurocognitive testing using computational psychiatry-A systematic review for ADHD. Psychol Bull 147:169–231.
25. Ging-Jehli NR, Arnold LE, Roley-Roberts ME, deBeus R (2022): Characterizing underlying cognitive components of ADHD presentations and co-morbid diagnoses: A diffusion decision model analysis. J Atten Disord 26:706–722.
26. Ging-Jehli NR, Kraemer HC, Eugene Arnold L, Roley-Roberts ME, deBeus R (2023): Cognitive markers for efficacy of neurofeedback for attention-deficit hyperactivity disorder – Personalized medicine using computational psychiatry in a randomized clinical trial. J Clin Exp Neuropsychol 45:118–131.
27. Ossola P, Pike AC (2023): Editorial: What is computational psychopathology, and why do we need it? Neurosci Biobehav Rev 152: 105170.
28. Pedersen ML, Ironside M, Amemori KI, McGrath CL, Kang MS, Graybiel AM, *et al.* (2021): Computational phenotyping of brain-behavior dynamics underlying approach-avoidance conflict in major depressive disorder. PLoS Comput Biol 17:e1008955.
29. Ratcliff R, Scharre DW, McKoon G (2022): Discriminating memory disordered patients from controls using diffusion model parameters from recognition memory. J Exp Psychol Gen 151:1377–1393.
30. Wiecki TV, Antoniades CA, Stevenson A, Kennard C, Borowsky B, Owen G, *et al.* (2016): A computational cognitive biomarker for early-stage Huntington's disease. PLoS One 11:e0148409.
31. Ging-Jehli NR, Arnold LE, Van Zandt T (2023): Cognitive-attentional mechanisms of cooperation-with implications for attention-deficit hyperactivity disorder and cognitive neuroscience. Cogn Affect Behav Neurosci 23:1545–1567.
32. Fried EI, Flake JK, Robinaugh DJ (2022): Revisiting the theoretical and methodological foundations of depression measurement. Nat Rev Psychol 1:358–368.
33. Kirlic N, Young J, Aupperle RL (2017): Animal to human translational paradigms relevant for approach avoidance conflict decision making. Behav Res Ther 96:14–29.
34. Letkiewicz AM, Kottler HC, Shankman SA, Cochran AL (2023): Quantifying aberrant approach-avoidance conflict in psychopathology: A review of computational approaches. Neurosci Biobehav Rev 147:105103.
35. Lewin K (1935): A Dynamic Theory of Personality. New York, NY: McGraw-Hill.
36. Loijen A, Vrijsen JN, Egger JIM, Becker ES, Rinck M (2020): Biased approach-avoidance tendencies in psychopathology: A systematic review of their assessment and modification. Clin Psychol Rev 77: 101825.
37. Miller NE (1959): Liberalization of basic S-R concepts: Extensions to conflict behavior, motivation and social learning. In: Koch S, editor. Psychology: A Study of a Science. General and Systematic Formulations, Learning, and Special Processes. New York: McGraw-Hill, 196–292.
38. Ironside M, Amemori K-I, McGrath CL, Pedersen ML, Kang MS, Amemori S, *et al.* (2020): Approach-avoidance conflict in major depressive disorder: Congruent neural findings in humans and nonhuman primates. Biol Psychiatry 87(5):399–408.
39. Livermore JJA, Klaassen FH, Bramson B, Hulsman AM, Meijer SW, Held L, *et al.* (2021): Approach-avoidance decisions under threat: The role of autonomic psychophysiological states. Front Neurosci 15:621517.
40. Der-Avakian A, Markou A (2012): The neurobiology of anhedonia and other reward-related deficits. Trends Neurosci 35:68–77.
41. Rizvi SJ, Pizzagalli DA, Sproule BA, Kennedy SH (2016): Assessing anhedonia in depression: Potentials and pitfalls. Neurosci Biobehav Rev 65:21–35.
42. Ariely D, Huber J, Wertenbroch K (2005): When do losses loom larger than gains? J Mark Res 42:134–138.
43. Davis AL, Jehli N, Miller JH, Weber RA (2015): Generosity across contexts. Rochester, NY: Social Science Research Network; 2015 Mar [cited 2022 Jun 1]. Report No.: 2592357. Available at: https://papers.ssrn.com/abstract=2592357. Accessed June 1, 2022.
44. Kahneman D, Tversky A (1979): Prospect theory: An analysis of decision under risk. Econometrica 47:263–291.
45. Novemsky N, Kahneman D (2005): The boundaries of loss aversion. J Mark Res 42:119–128.
46. Deakin JFW, Graeff FG (1991): 5-HT and mechanisms of defence. J Psychopharmacol 5:305–315.
47. Hagura N, Haggard P, Diedrichsen J (2017): Perceptual decisions are biased by the cost to act. eLife 6:e18422.
48. Capra CM, Croson RT, Rigdon ML, Rosenblat TS (2020): Handbook of Experimental Game Theory. Cheltenham, UK: Edward Elgar Publishing.
49. Ratcliff R, Smith PL (2004): A comparison of sequential sampling models for two-choice reaction time. Psychol Rev 111:333–367.
50. Van Zandt T, Ratcliff R (1995): Statistical mimicking of reaction time data: Single-process models, parameter variability, and mixtures. Psychon Bull Rev 2:20–54.
51. Cartwright D, Festinger L (1943): A quantitative theory of decision. Psychol Rev 50:595–621.

52. Forstmann BU, Ratcliff R, Wagenmakers EJ (2016): Sequential sampling models in cognitive neuroscience: Advantages, applications, and extensions. Annu Rev Psychol 67:641–666.
53. Smith PL, Ratcliff R (2015): An introduction to the diffusion model of decision making. In: Forstmann BU, Wagenmakers EJ, editors. An Introduction to Model-Based Cognitive Neuroscience. New York, NY: Springer, 49–70.
54. Ratcliff R (1978): A theory of memory retrieval. Psychol Rev 85:59–108.
55. Moughrabi N, Botsford C, Gruichich TS, Azar A, Heilicher M, Hiser J, *et al.* (2022): Large-scale neural network computations and multivariate representations during approach-avoidance conflict decision-making. Neuroimage 264:119709.
56. Paulus MP (2020): Driven by pain, not gain: Computational approaches to aversion-related decision making in psychiatry. Biol Psychiatry 87:359–367.
57. Smith R, Kirlic N, Stewart JL, Touthang J, Kuplicki R, Khalsa SS, *et al.* (2021): Greater decision uncertainty characterizes a transdiagnostic patient sample during approach-avoidance conflict: A computational modelling approach. J Psychiatry Neurosci 46:E74–E87.
58. Smith R, Kirlic N, Stewart JL, Touthang J, Kuplicki R, McDermott TJ, *et al.* (2021): Long-term stability of computational parameters during approach-avoidance conflict in a transdiagnostic psychiatric patient sample. Sci Rep 11:11783.
59. Talmi D, Dayan P, Kiebel SJ, Frith CD, Dolan RJ (2009): How humans integrate the prospects of pain and reward during choice. J Neurosci 29:14617–14626.
60. Chu S, Hutcherson C, Ito R, Lee ACH (2023): Elucidating medial temporal and frontal lobe contributions to approach-avoidance conflict decision-making using functional MRI and the hierarchical drift diffusion model. Cereb Cortex 33:7797–7815.
61. Rolle CE, Pedersen ML, Johnson N, Amemori KI, Ironside M, Graybiel AM, *et al.* (2022): The role of the dorsal–lateral prefrontal cortex in reward sensitivity during approach–avoidance conflict. Cereb Cortex 32:1269–1285.
62. Fengler A, Govindarajan LN, Chen T, Frank MJ (2021): Likelihood approximation networks (LANs) for fast inference of simulation models in cognitive neuroscience. eLife 10:e65074.
63. Fengler A, Bera K, Pedersen ML, Frank MJ (2022): Beyond drift diffusion models: Fitting a broad class of decision and reinforcement learning models with HDDM. J Cogn Neurosci 34:1780–1805.
64. Bowman NE, Kording KP, Gottfried JA (2012): Temporal integration of olfactory perceptual evidence in human orbitofrontal cortex. Neuron 75:916–927.
65. Cisek P, Puskas GA, El-Murr S (2009): Decisions in changing conditions: The urgency-gating model. J Neurosci 29:11560–11571.
66. Ditterich J (2006): Evidence for time-variant decision making. Eur J Neurosci 24:3628–3641.
67. Thura D, Beauregard-Racine J, Fradet CW, Cisek P (2012): Decision making by urgency gating: Theory and experimental support. J Neurophysiol 108:2912–2930.
68. Bogacz R, Brown E, Moehlis J, Holmes P, Cohen JD (2006): The physics of optimal decision making: A formal analysis of models of performance in two-alternative forced-choice tasks. Psychol Rev 113:700–765.
69. Beck AT, Steer RA, Brown G (1996): Beck Depression Inventory–II. American Psychological Association. Available at: http://doi.apa.org/getdoi.cfm?doi=10.1037/t00742-000. Accessed January 24, 2023.
70. Furukawa TA (2010): Assessment of mood: Guides for clinicians. J Psychosom Res 68:581–589.
71. Smarr KL, Keefer AL (2020): Measures of depression and depressive symptoms. Arthritis Care Res 72(suppl 10):608–629.
72. Snaith RP, Hamilton M, Morley S, Humayan A, Hargreaves D, Trigwell P (1995): A scale for the assessment of hedonic tone the Snaith–Hamilton pleasure scale. Br J Psychiatry 167:99–103.
73. Nakonezny PA, Carmody TJ, Morris DW, Kurian BT, Trivedi MH (2010): Psychometric evaluation of the Snaith–Hamilton pleasure scale in adult outpatients with major depressive disorder. Int Clin Psychopharmacol 25:328–333.
74. Trøstheim M, Eikemo M, Meir R, Hansen I, Paul E, Kroll SL, *et al.* (2020): Assessment of anhedonia in adults with and without mental illness: A systematic review and meta-analysis. JAMA Netw Open 3:e2013233.
75. Watson D, Clark LA, Tellegen A (1988): Development and validation of brief measures of positive and negative affect: The Panas scales. J Pers Soc Psychol 54:1063–1070.
76. Stern RA, Arruda JE, Hooper CR, Wolfner GD, Morey CE (1997): Visual analogue mood scales to measure internal mood state in neurologically impaired patients: Description and initial validity evidence. Aphasiology 11:59–71.
77. Clark LA, Watson D (1991): Tripartite model of anxiety and depression: Psychometric evidence and taxonomic implications. J Abnorm Psychol 100:316–336.
78. Ottenbreit ND, Dobson KS (2004): Avoidance and depression: The construction of the Cognitive–Behavioral Avoidance Scale. Behav Res Ther 42:293–313.
79. Wiecki TV, Sofer I, Frank MJ (2013): HDDM: Hierarchical Bayesian estimation of the Drift-Diffusion Model in Python. Front Neuroinform 7:14.
80. Sherdell L, Waugh CE, Gotlib IH (2012): Anticipatory pleasure predicts motivation for reward in major depression. J Abnorm Psychol 121:51–60.
81. Lawlor VM, Webb CA, Wiecki TV, Frank MJ, Trivedi M, Pizzagalli DA, Dillon DG (2020): Dissecting the impact of depression on decision-making. Psychol Med 50:1613–1622.
82. Pizzagalli DA, Iosifescu D, Hallett LA, Ratner KG, Fava M (2008): Reduced hedonic capacity in major depressive disorder: Evidence from a probabilistic reward task. J Psychiatr Res 43:76–87.
83. Garcia-Guerrero S, O'Hora D, Zgonnikov A, Scherbaum S (2023): The action dynamics of approach-avoidance conflict during decision-making. Q J Exp Psychol (Hove) 76:160–179.
84. Kessler RC, Adler L, Barkley R, Biederman J, Conners CK, Demler O, *et al.* (2006): The prevalence and correlates of adult ADHD in the United States: Results from the national comorbidity survey replication. Am J Psychiatry 163:716–723.
85. Wichers M, Jacobs N, Derom C, Thiery E, van Os J (2007): Depression: Too Much Negative Affect or Too Little Positive Affect? Twin Res Hum Genet 10(suppl1):19–20.
86. Mehrabian A (1997): Comparison of the PAD and PANAS as models for describing emotions and for differentiating anxiety from depression. J Psychopathol Behav Assess 19:331–357.
87. Watson D, Weber K, Assenheimer JS, Clark LA, Strauss ME, McCormick RA (1995): Testing a tripartite model: I. Evaluating the convergent and discriminant validity of anxiety and depression symptom scales. J Abnorm Psychol 104:3–14.
88. Watson D, Clark LA (1991): Mood and anxiety symptom questionnaire. American Psychological Association. Available at: http://doi.apa.org/getdoi.cfm?doi=10.1037/t13679-000. Accessed January 24, 2023.
89. Zevon MA, Tellegen A (1982): The structure of mood change: An idiographic/nomothetic analysis. J Pers Soc Psychol 43:111–122.
90. Thayer RE (1996): The Origin of Everyday Moods: Managing Energy, Tension, and Stress. Oxford: Oxford University Press.
91. Garland EL, Atchley RM, Hanley AW, Zubieta JK, Froeliger B (2019): Mindfulness-Oriented Recovery Enhancement remediates hedonic dysregulation in opioid users: Neural and affective evidence of target engagement. Sci Adv 5:eaax1569.
92. Winer ES, Jordan DG, Collins AC (2019): Conceptualizing anhedonias and implications for depression treatments. Psychol Res Behav Manag 12:325–335.
93. Ging-Jehli NR, Painter QA, Kraemer HA, Roley-Roberts ME, Panchyshyn C, deBeus R, Arnold LE (2024): A diffusion decision model analysis of the cognitive effects of neurofeedback for ADHD. Neuropsychology 38:146–156.
94. American Psychiatric Association (2013): Diagnostic and Statistical Manual of Mental Disorders, 5th ed. Washington, DC: American Psychiatric Publishing.
95. McIntosh D, Kutcher S, Binder C, Levitt A, Fallu A, Rosenbluth M (2009): Adult ADHD and comorbid depression: A consensus-derived diagnostic algorithm for ADHD. Neuropsychiatr Dis Treat 5:137–150.

SUPPLEMENTARY INFORMATION

Cognitive Signatures of Depressive and Anhedonic Symptoms, and Affective States, Using Computational Modeling and Neurocognitive Testing

Ging-Jehli *et al.*

Supplementary Materials

Ethics

All procedures of this work comply with the ethical standards of the relevant national and institutional committees on human experimentation and with the Helsinki Declaration of 1975 (1).

Study procedures

After the participant provided consent, the experimenter attached two rectangular surface electrodes (Coulburn Instruments, Holliston, MA, USA) to the participant's right ankle. A calibration determined 10 stimulus intensities that induced shock levels from *a slightly uncomfortable feeling that would still affect decision-making in the task* (shock level 1) to *a highly aversive (but not painful) feeling* (shock level 10). After calibration, participants received task instructions displayed on a computer screen.

Shock calibration

Electrical stimulation was generated by a Digitimer DG2A Train/Delay generator (Digitimer, Welwyn Garden City, UK) that generated pulse trains of 500ms at 50Hz and delivered shocks at this frequency via a DS8R (Digitimer DS8R Biphasic Constant Current Stimulator, Digitimer, Welwyn Garden City, UK). The two electrodes attached to the participant's right ankle were used for stimulation.

At the beginning of the shock level calibration procedure, participants were instructed that the procedure determines their individual level 1 stimulation (minimum) and level 10 stimulation (maximum). Participants were told that level 1 should be slightly uncomfortable (like a light pinch) but still carry some weight in their decision-making and that level 10 should be maximally uncomfortable without being painful. The calibration procedure started by applying a 1mA stimulation and then proceeding in steps of 1mA (or smaller increments if necessary) until the

participant expressed that the stimulation was slightly uncomfortable. At this point, participants were asked how they would feel about taking the slightly uncomfortable stimulation for 5 cents, to determine whether this level of stimulation carried some weight in their decision-making. If they reported that they would take this offer (stimulation level in question for 5 cents) 40% to 60% of the time (demonstrating that this stimulation carried some weight) this level was chosen as level 1. Once the level 1 was determined, stimulation was gradually increased in intensity to determine the level 10. The stimulation was increased in intensity until the participant reported that the stimulation resulted in their maximum level of discomfort (that they would be willing to take during the task) without being painful. At this point, they were asked how they would feel about taking the highly uncomfortable stimulation for additional 5 to 50 cents. If they reported that they would take this offer 40% to 60% of the time (demonstrating that this carried some weight) this level was chosen as the level 10. In cases where participants offered responses that seemed inconsistent (such as agreeing to endure greater electric shocks for smaller monetary rewards than for larger shocks) or indicated changes in their willingness to accept a particular shock level for a given monetary incentive, we either re-administered the calibration process or made necessary adjustments to individual shock levels. Next, participants completed 15 practice trials of the task while supervised by the experimenter, allowing for readjustment of the shock level calibration in case participants should choose approach on all practice trials.

Additional Task details

The task was implemented in Psychtoolbox running on MATLAB 2020a. Shock intensity was controlled via MATLAB on the DS8R stimulation device, which was triggered via Matlab and a NI DAQ USB-6009 device (National Instruments, Austin, TX, USA) that triggered the DG2A train generator.

Participants used a joystick to indicate their responses. Specifically, on Pavlovian response congruent trials, approach decisions were indicated by pulling the joystick. On Pavlovian response incongruent trials, approach decisions were indicated by pushing the joystick. Pavlovian response congruent and incongruent trials were counterbalanced. For each presented offer, we collected participants' choice and RTs that served as inputs into our computational models.

The adaptive approach avoidance task (aAAC) is a novel task based on prior work in humans (2) and non-human primates (3). The aAAC was optimized to induce individually calibrated levels for aversion and used a trial-by-trial adaptive procedure to optimally induce variable levels of approach-avoidance conflict. Moreover, ecologically valid stimuli (i.e., physically aversive stimulation and monetary rewards) were introduced to generate individually adjusted degrees of conflict. The aAAC task's design allows one to induce approach-avoidance conflict on a reward-aversion continuum with varying degrees of conflict, while adjusting for individual decision indifference points within this continuum.

Offers were dynamically created on a trial-by-trial case and for each participant separately. Specifically, the first nine trials were randomly sampled from the reward-aversion space (i.e., rewards and aversion could each range from 10 to 100, in steps of 10). Afterwards, we estimated for each subsequent trial and for each participant their momentary indifference curve along which subjects are equally likely to approach or avoid. To do so, we used logistic regression and all choices (up to and excluding the current trial) as dependent variable (1=approach, 0=avoid) and the corresponding reward and aversion as independent variables. The offer for the current trial was then created by randomly sampling either with a probability of 0.4 from a range of the reward-aversion space that was close to the estimated indifference curve, with a probability of 0.3 from a range of the reward-aversion space that was farther away from the estimated indifference curve,

or at pseudo-random with a probability of 0.3 from a range of space that lay in a 3x3 grid across the reward-aversion space. Specifically, subsequent trials were selected with respect to the decision boundary as follows: 30% "random" as above, 30% "variable" (following a Gaussian distribution of the normalized distance to boundary, $\mathcal{N}_d(0, 20\%)$) and 40% "close" ($\mathcal{N}_d(0, 5\%)$).

Response symbols and offers were simultaneously presented for 4 seconds. When participants made a choice, the circle was locked at the target until the 4s were up. A fixation cross was then presented and if participants decided to approach an offer, they were administered the corresponding shock level for 500ms during this period (jittered after fixation cross onset, range 0.5-10s; mean 1.77s). Following, participants received 2s feedback about the number of cents they earned in this trial (0 in case of avoid or no-response).

Description of different versions of sequential sampling models

Similarities and differences between these model versions have already been extensively discussed elsewhere (4–9).

Diffusion Decision Model (DDM). The DDM (10) assumes fixed decision boundaries and a path of evidence accumulation that follows a noisy Wiener process with a mean (known as drift rate) and a variance (known as diffusion coefficient). The model includes within-trial noise variability (s). Drift rate v is normally distributed with standard deviation η, and nondecision time component (Ter) and starting point (z) are assumed to be uniformly distributed with ranges s_t and s_z, respectively.

Ornstein-Uhlenbeck Model (OUM). The OUM (11) assumes fixed decision boundaries like the DDM. In contrast to the DDM, it assumes noisy evidence accumulation with a drift rate that is either leaky (less accumulation) or attractive (more accumulation) as the decision particle approaches the bound.

Angle Boundary Model (ABM). The ABM is a popular modification of the DDM, assuming linearly collapsing decision boundaries over time (6,12,13). Collapsing boundaries are used to model the need for less signal strength in evidence accumulation to commit to a response as time passes, such as when participants become increasingly impatient, when externally or internally imposed response deadlines are imposed, or urgency signals become more pressing (14–17). Moreover, the ABM is known to provide better fits than the classic DDM in some cases (12,13,18,19).

Weibull Boundary Model (WBM). The WBM is a popular modification of the DDM, assuming collapsing decision boundaries like the ABM. In contrast to the ABM, the WBM includes a Weibull-informed collapse that is determined by two parameters determining the shape and rate of the collapse, respectively (19–22).

Details about model comparison

We focused on the following four SSM versions: the DDM (10), OUM (11), ABM (23), and the WBM (20). Supplemental Table S2 provides specifications of these regression equations for all SSMs by following the conventional notations for mixed-effect regression models in the *lme4* and *brms* packages in R (24–26). To find the model that accounts best for data from our AAC task, we proceeded in two steps:

Comparison between SSM versions. Pedersen et al. (27) identified a best-fitting DDM for behavioral data from a similar AAC task. We therefore used their model (i.e., parameter specification) as the baseline for comparison with different SSM versions (e.g., DDM, collapsing bounds).

Comparison within best SSM version. After establishing the best SSM version, we explored whether different parameter specifications would additionally improve the absolute model fit. We

selected the SSM version with the best fitting parameter specification, in terms of both deviance information criterion (DIC) and posterior predictive checks. This allowed us to account for the fact that the specifics of our AAC task (e.g., response-adaptive creation of offers across trials, individual-specific levels of electric stimulation as the aversive component of offers) differed from those in Pedersen et al. (27).

Fitting Procedure

We fit SSMs to data within a Bayesian hierarchical framework implemented through HDDM. Hence, the coefficients of the mixed-effect regressions of each model parameter (specified in Supplementary Table S2) were estimated separately for each participant, but where each participant was assumed to be drawn from a distribution across all participants (28). Hierarchical estimation improves parameter recovery and out of sample prediction, in general and for SSMs in particular (29,30). Model predictors were normalized before entering the regressions (except dummy-coded predictors). Models were run with 3 chains, each with 10,000 samples (including 5,000 samples as burn-in). We used the empirically-sourced and weakly informative priors from HDDM for all models (21,30). We ensured model convergence by examining trace plots and the Gelman-Rubin $\hat{R}$ statistic, which was below the threshold of 1.1 for all model parameters, indicating sufficient chain mixing and model convergence (31).

Supplemental References

1. World Medical Association. Declaration of Helsinki: Ethical principles for medical research involving human subjects. J Am Med Assoc. 1975;284(23):3043–5.
2. Ironside M, Amemori K ichi, McGrath CL, Pedersen ML, Kang MS, Amemori S, et al. Approach-Avoidance Conflict in Major Depressive Disorder: Congruent Neural Findings in Humans and Nonhuman Primates. Biol Psychiatry. 2020 Mar 1;87(5):399–408.
3. Amemori K ichi, Graybiel AM. Localized microstimulation of primate pregenual cingulate cortex induces negative decision-making. Nat Neurosci. 2012 May;15(5):776–85.

4. Bogacz R, Brown E, Moehlis J, Holmes P, Cohen JD. The physics of optimal decision making: A formal analysis of models of performance in two-alternative forced-choice tasks. Psychol Rev. 2006;113:700–65.

5. Fengler A, Bera K, Pedersen ML, Frank MJ. Beyond Drift Diffusion Models: Fitting a Broad Class of Decision and Reinforcement Learning Models with HDDM. J Cogn Neurosci. 2022 Sep 1;34(10):1780–805.

6. Forstmann BU, Ratcliff R, Wagenmakers EJ. Sequential Sampling Models in Cognitive Neuroscience: Advantages, Applications, and Extensions. Annu Rev Psychol. 2016 Jan 4;67(1):641–66.

7. Ging-Jehli NR, Ratcliff R, Arnold LE. Improving neurocognitive testing using computational psychiatry—A systematic review for ADHD. Psychol Bull. 2021;147(2):169–231.

8. Ratcliff R, Smith PL. A Comparison of Sequential Sampling Models for Two-Choice Reaction Time. Psychol Rev. 2004;111(2):333–67.

9. Van Zandt T. How to fit a response time distribution. Psychon Bull Rev. 2000 Sep 1;7(3):424–65.

10. Ratcliff R. A theory of memory retrieval. Psychol Rev. 1978;85(2):59–108.

11. Busemeyer JR, Townsend JT. Fundamental derivations from decision field theory. Math Soc Sci. 1992 Jun 1;23(3):255–82.

12. Doya K, Ishii S, Pouget A. Bayesian Brain: Probabilistic Approaches to Neural Coding. MIT Press; 2007. 341 p.

13. Voss A, Lerche V, Mertens U, Voss J. Sequential sampling models with variable boundaries and non-normal noise: A comparison of six models. Psychon Bull Rev. 2019 Jun 1;26(3):813–32.

14. Bowman NE, Kording KP, Gottfried JA. Temporal Integration of Olfactory Perceptual Evidence in Human Orbitofrontal Cortex. Neuron. 2012 Sep 6;75(5):916–27.

15. Cisek P, Puskas GA, El-Murr S. Decisions in Changing Conditions: The Urgency-Gating Model. J Neurosci. 2009 Sep 16;29(37):11560–71.

16. Ditterich J. Evidence for time-variant decision making. Eur J Neurosci. 2006;24(12):3628–41.

17. Thura D, Beauregard-Racine J, Fradet CW, Cisek P. Decision making by urgency gating: theory and experimental support. J Neurophysiol. 2012 Dec;108(11):2912–30.

18. Drugowitsch J, Moreno-Bote R, Churchland AK, Shadlen MN, Pouget A. The Cost of Accumulating Evidence in Perceptual Decision Making. J Neurosci. 2012 Mar 14;32(11):3612–28.

19. Hawkins GE, Forstmann BU, Wagenmakers EJ, Ratcliff R, Brown SD. Revisiting the Evidence for Collapsing Boundaries and Urgency Signals in Perceptual Decision-Making. J Neurosci. 2015 Feb 11;35(6):2476–84.

20. Churchland AK, Kiani R, Shadlen MN. Decision-making with multiple alternatives. Nat Neurosci. 2008 Jun;11(6):693–702.

21. Fengler A, Govindarajan LN, Chen T, Frank MJ. Likelihood approximation networks (LANs) for fast inference of simulation models in cognitive neuroscience. Wyart V, Behrens TE, Acerbi L, Daunizeau J, editors. eLife. 2021 Apr 6;10:e65074.

22. Hanks TD, Mazurek ME, Kiani R, Hopp E, Shadlen MN. Elapsed Decision Time Affects the Weighting of Prior Probability in a Perceptual Decision Task. J Neurosci. 2011 Apr 27;31(17):6339–52.

23. Forstmann BU, Ratcliff R, Wagenmakers EJ. Sequential Sampling Models in Cognitive Neuroscience: Advantages, Applications, and Extensions. Annu Rev Psychol. 2016;67(1):641–66.

24. Bates D, Märchler M, Bolker B, Walker S. Fitting Linear Mixed-Effects Models Using lme4. Jornal of Statistical Software. 2015;67(1):1–48.

25. Bürkner PC. brms: An R Package for Bayesian Multilevel Models Using Stan. J Stat Softw. 2017 Aug 29;80:1–28.

26. R Core Team. R: A language and environment for statistical computing [Internet]. Vienna, Austria: R Foundation for Statistical Computing; 2021. Available from: https://www.R-project.org/

27. Pedersen ML, Ironside M, Amemori K ichi, McGrath CL, Kang MS, Graybiel AM, et al. Computational phenotyping of brain-behavior dynamics underlying approach-avoidance conflict in major depressive disorder. PLOS Comput Biol. 2021 May 10;17(5):e1008955.

28. Gelman A, Hill J. Data Analysis Using Regression and Multilevel/Hierarchical Models. Cambridge University Press; 2006. 651 p.

29. Boehm U, Marsman M, Matzke D, Wagenmakers EJ. On the importance of avoiding shortcuts in applying cognitive models to hierarchical data. Behav Res Methods. 2018 Aug 1;50(4):1614–31.

30. Wiecki T, Sofer I, Frank M. HDDM: Hierarchical Bayesian estimation of the Drift-Diffusion Model in Python. Front Neuroinformatics [Internet]. 2013 [cited 2022 Mar 24];7. Available from: https://www.frontiersin.org/article/10.3389/fninf.2013.00014

31. Gelman A, Rubin DB. Inference from Iterative Simulation Using Multiple Sequences. Stat Sci. 1992;7(4):457–72.

Supplementary Tables

Supplementary Table S1. *Sample Characteristics.*

Variables	Mean/Ratio	SD	Min	Max
Demographics				
Age (in years)	28.79	7.43	18	44
Sex (Male:Female)	13:35	na	na	na
Clinical Measures				
PANAS Total Score	43.44	9.67	26	64
PANAS-PA	29.13	9.23	13	49
PANAS-NA	14.31	5.51	10	33
VAMS - Friendly To Hostile	25.79	21.79	0	71
VAMS - Happy To Sad	27.85	21.46	0	71
VAMS - Tense To Relax	58.33	23.01	23	100
BDI-II	10.81	9.46	0	41
SHAPS	22.73	6.14	14	38
MASQ Total Score	115.73	33.17	69	204
MASQ-GDA	18.10	6.32	11	39
MASQ-AA	21.31	5.54	17	43
CBAS Total Score	58.83	20.91	32	124
CBAS-BS	15.73	6.75	8	38
CBAS-BN	12.23	4.69	6	25
CBAS-CS	12.98	5.45	7	28
CBAS-CN	17.9	7.08	10	37
Task Performance Summary Statistics				
Mean Reaction Times (in ms)	1593	343	725	2251
Approach Frequency	0.72	0.14	0.48	1
Presented Reward	45.92	25.92	10	100
Presented Aversion	62.78	26.29	10	100
Amount of Received Shock (in mA)	6.93	4.68	0.6	22

Note. Table is based on N=48 as the questionnaire data of two subjects was missing (see Methods). SD refers to the standard deviations of the means between subjects. Min refers to the minimum mean across subjects. Max refers to the maximum mean across subjects. We refer to the Methods for a description of measures and interpretation of scores. Abbreviations: PANAS = Positive and Negative Affect Schedule; SHAPS = Snaith-Hamilton Pleasure Scale; BDI = Beck Depression Inventory; VAMS = Visual Analogue Mood Scale; CBAS = Cognitive and Behavioral Avoidance Scale; MASQ = Mood and Anxiety Symptom Questionnaire (GDA and AA are the anxiety-related subscores). Three participants met the criteria for major depressive disorder according to the BDI.

Supplementary Table S2. *Comparison of different versions and specifications of sequential sampling models (SSMs).*

Model descriptions			Parameter specifications				
Model	Version	DIC	Drift rate (v)	Boundary separation (a)	Starting point (z)	Nondecision Time (Ter)	Version-specific parameters
Part II: within-model-specification comparison of selected model							
best	abm	9005	1 + (rewardLog + averse)*cD	1 + conflict	1 + PB	1	θ ~ 1 + conflict
2	abm	9010	1 + (reward + averse)*cD	1 + conflict*cD	1	1	θ ~ 1
3	abm	9013	1 + (rewardLog + averse)*cD	1 + conflict	1 + PB	1	θ ~ 1
4	abm	9024	1 + (rewardLog + averse)*cD	1 + conflict*cD	1	1	θ ~ 1 + conflict*cD
5	abm	9045	1 + (rewardLog + averse)*cD	1 + conflict	1	1	θ ~ 1
6	abm	9436	1 + rewardLog*averse	1 + conflict	1	1	θ ~ 1
7	abm	9438	1 + rewardLog*averse	1 + conflict	1	1	1 + conflict
Part I: between-model-version comparison with base specification							
8	**abm**	**9526**	**1 + rewardLog + averse**	**1 + conflict**	**1 + PB**	**1**	**θ ~ 1**
9	**wbm**	**9669**	**1 + rewardLog + averse**	**1 + conflict**	**1 + PB**	**1**	**α ~ 1; β ~ 1**
baseline	**ddm**	**10095**	**1 + rewardLog + averse**	**1 + conflict**	**1 + PB**	**1**	
11	**oum**	**10547**	**1 + rewardLog + averse**	**1 + conflict**	**1 + PB**	**1**	**δ ~ 1**

Note. Different SSMs (one model per row) with the best-fitting model represented in the first row (see Methods for details). Continuous variables were mean-centered at the subject-level before entering into the regression. We follow standard notation of regression-based models (i.e., y ~ x*z ⇔ y ~ 1 + x + z + x*z). *cD* indicates a dummy variable to distinguish between offers with positive (cD=1) and negative (cD=0) net values. *PB* indicates a dummy variable to distinguish between Pavlovian response-congruent and response-incongruent trials. *abm* refers to models with a linearly collapsing boundary with parameter *theta* indicating the angle of the collapse. *ddm* refers to the diffusion decision model that was used by Pedersen et al. (2021) and that served as a baseline. *wbm* refers to models with Weibull-informed collapsing boundaries with parameters α indicating the rate of the collapse and *β* indicating the shape of the collapse. *ou* refers to the Ornstein-Uhlenbeck model with *δ* indicating the decay parameter of diffusion processes. *Constant* refers to one constant parameter throughout the task. *1* refers to intercepts. *DIC* refers to the deviance information criterion. We refer to the Supplement for posterior predictive checks (PPCs).

Supplementary Table S3. *Additional Comparisons of different versions and specifications of sequential sampling model (SSMs).*

Model descriptions			Parameter specifications				
Model	Version	DIC	Drift rate (v)	Boundary separation (a)	Starting point (z)	Nondecision Time (Ter)	Model version-specific parameters
1	abm	9445	1 + reward*averse	1 + conflict	1	1	θ ~ 1
2	abm	9446	1 + reward*averse	1 + conflict	1	1	1 + conflict
3	abm	9547	1 + rewardLog + averse	1 + conflict	1	1	θ ~ 1
4	abm	9629	1 + reward + averse	1 + conflict	1	1	θ ~ 1 + conflict
5	abm	9636	1 + reward + averse	1 + conflict	1	1	θ ~ 1
6	abm	9670	1 + reward + averse	1	1	1	θ ~ 1
7	ddm	9499	1 + rewardLog + averse	1 + conflict	1	1	s_t ~ 1; s_z ~ 1; η ~1
8	ddm	9508	1 + reward + averse	1 + conflict	1	1	s_t ~ 1; s_z ~ 1; η ~1
9	ddm	9590	1 + reward + averse	1	1	1	s_t ~ 1; s_z ~ 1; η ~1
10	wbm	9679	1 + rewardLog +averse	1 + conflict	1	1	a ~ 1; β ~ 1
11	wbm	9776	1 + reward +averse	1	1	1	a ~ 1; β ~ 1 + conflict
12	wbm	9796	1 + reward + averse	1	1	1	A ~ 1 + conflict; β ~ 1
13	wbm	9795	1 + reward + averse	1 + conflict	1	1	α ~ 1; β ~ 1
14	oum	10559	1 + rewardLog + averse	1 + conflict	1	1	δ ~ 1
15	oum	10664	1 + reward + averse	1	1	1	δ ~ 1
16	oum	10634	1 + reward + averse	1 + conflict	1	1	δ ~ 1
17	oum	n.a.	1 + reward + averse	1	1	1	δ ~ 1 + conflict

Note. Different SSMs (one model per row) that are detailed in the Methods of the main manuscript. Continuous variables were mean-centered at the subject-level before entering the regression. We follow standard notation of regression-based models (i.e., y ~ x*z ⇔ y ~ 1 + x + z + x*z). *cD* indicates a dummy variable to distinguish between offers with positive (cD=1) and negative (cD=0) net values. *PB* indicates a dummy variable to distinguish between Pavlovian congruent (PB=1) and incongruent (PB=0) trials. *abm* refers to models with a linearly collapsing boundary with parameter *theta* indicating the angle of the collapse. ddm refers to the classical diffusion decision model with parameters s_t indicating variability in nondecision time; s_z indicating variability in starting point; *η* indicating across-trial variability in drift rate. *weibull* refers to models with Weibull-informed collapsing boundaries with parameters α indicating the rate of the collapse and *β* indicating the shape of the collapse. *ou* refers to the Ornstein-uhlenbeck model with *δ* indicating the decay parameter of diffusion processes. *Constant* refers to one constant parameter throughout the task. *1* refers to intercepts. *DIC* refers to the deviance information criterion. Posterior predictive checks of selected models are shown in Supplementary Figure S2.

Supplementary Table S4. *Posterior distributions (means and corresponding) credible intervals of group estimates for the best-fitting model.*

Parameter	Coefficient	Mean	Lower	Upper
drift rate (v)	intercept	0.437	0.207	0.678
	cD(positive)	0.801	0.590	1.011
	reward	0.604	0.528	0.677
	aversion	-0.536	-0.624	-0.447
	reward:cD(positive)	-0.410	-0.490	-0.331
	aversion:cD(positive)	0.247	0.140	0.354
boundary separation (a)	intercept	1.874	1.719	2.048
	conflict	-0.035	-0.069	-0.004
starting point bias (zBias)	intercept	0.552	0.524	0.580
	PB(incongruent)	0.003	-0.014	0.019
rate of linear collapse (θ)	intercept	0.546	0.489	0.600
	conflict	-0.031	-0.055	-0.008
nondecision time (Ter)	intercept	0.634	0.574	0.693

Note. Lower and Upper refer to the corresponding bounds of the 95% highest density intervals of the posterior group distribution. cD refers to the domains (positive, negative) while PB refers to the Pavlovian response incongruent/congruent trials.

Supplementary Table S5. *Regression Coefficients of model parameters on Depression severity (BDI total score) and Anhedonia severity (SHAPS total score), negative affect severity (PANAS-NA score), and tension severity (VAMS sadness score).*

	Model 1 (M1)			Model 2 (M2)			Model 3 (M3)			Model 4 (M4)		
Variables	*B*	*SE*	*P*	*B*	*SE*	*P*	*B*	*SE*	*P*	*B*	*SE*	*P*
Dependent Variable: bdi total score												
Constant	0.000	0.136	1.000	0.000	0.137	1.000	0.000	0.131	1.000	-0.013	0.134	0.921
Ter	**0.037**	**0.137**	**0.011**				**0.319**	**0.134**	**0.022**	0.289	0.144	0.051
zBias_i				**-0.338**	**0.139**	**0.019**	**-0.286**	**0.134**	**0.038**	-0.255	0.144	0.084
Ter-by-zBias_i										-0.083	0.138	0.552
Adjusted R2	0.115			0.095			0.179			0.167		
Comparison M2 & M3: F(1, 46) = 5.668, p = 0.022												
Dependent Variable: shaps total score												
Constant	0.000	0.140	1.000	0.000	0.130	1.000	0.000	0.128	1.000	0.031	0.128	0.809
Ter	0.274	0.142	0.060				0.205	0.131	0.125	0.276	0.138	0.052
zBias_i				**-0.451**	**0.132**	**0.001**	**-0.417**	**0.131**	**0.003**	**-0.490**	**0.139**	**0.001**
Ter-by-zBias_i										0.194	0.133	0.150
Adjusted R2	0.055						0.211			0.231		
Comparison M2 & M3: F(1,46) = 2.444, p=0.125												
Dependent Variable: PANAS negative affect												
Constant	0.000	0.134	1.000	0.000	0.138	1.000	0.000	0.131	1.000	-0.075	0.127	0.557
a	**-0.396**	**0.135**	**0.005**				**-0.339**	**0.136**	**0.016**	**-0.366**	**0.128**	**0.007**
zBias_c				**0.329**	**0.139**	**0.023**	0.251	0.136	0.070	0.137	0.135	0.318
a-by-zBias_c										**-0.335**	**0.131**	**0.014**
Adjusted R2	0.139			0.089			0.182			0.272		
Comparison M4 & M1: F(1, 45) = 5.226, p = 0.001												
Comparison M4 & M2: F(1, 45) = 6.808, p = 0.002												
Comparison M4 & M3: F(1, 45) = 6.581, p = 0.014												

Table continues.

Table continued.

	Model 1 (M1)			Model 2 (M2)			Model 3 (M3)			Model 4 (M4)		
Variables	*B*	*SE*	*P*	*B*	*SE*	*P*	*B*	*SE*	*P*	*B*	*SE*	*P*
Dependent Variable: VAMS tension												
Constant	0.000	0.138	1.000	0.000	0.140	1.000	0.000	0.135	1.000	-0.012	0.141	0.934
v_reward_neg	**0.334**	**0.139**	**0.020**				0.294	0.138	0.039	0.319	0.159	0.051
theta_conflict				**0.285**	**0.141**	**0.049**	0.235	0.138	0.096	0.225	0.143	0.124
v_reward_neg-by-theta_conflict										0.070	0.210	0.739
Adjusted R2	0.092			0.061			0.128			0.111		
Comparison M4 & M1: F(1, 46) = 1.473, p = 0.240												
Comparison M4 & M2: F(1, 46) = 2.269, p = 0.115												
Comparison M4 & M3: F(1, 46) = 0.112, p = 0.739												

Note. N=48. We examined the impact of nondecision time (Ter) and starting point bias for Pavlovian incongruent trials (zBias) on depression severity as measured by BDI total score (top part) and anhedonia severity as measured by SHAPS total score (bottom part). *p values* smaller than 0.05 are in bold. All variables were z-scored before entering the regression. We also estimated models with Ter-by-zBias interaction terms. However, these models did not provide evidence for any significant interactions and they were outperformed by M3 in terms of their ability to account for variability in the respective dependent variable.

Supplementary Table S6. *Regression Coefficients of mean reaction time and mean frequency of approach decisions on Depression severity (BDI total score) and Anhedonia severity (SHAPS total score), negative affect severity (PANAS-NA score), and tension severity (VAMS sadness score).*

	Model 1 (M1)			Model 2 (M2)			Model 3 (M3)			Model 4 (M4)		
Variables	*B*	*SE*	*P*	*B*	*SE*	*P*	*B*	*SE*	*P*	*B*	*SE*	*P*
Dependent Variable: BDI-II total score												
Constant	0.000	0.146	1.000	0.000	0.145	1.000	0.000	0.146	1.000	0.042	0.154	0.788
MRT	0.063	0.147	0.672				0.120	0.158	0.450	0.061	0.173	0.724
MF(AP)				0.017	0.146	0.429	0.160	0.158	0.316	0.211	0.170	0.219
MRT*MF(AP)										0.119	0.142	0.406
Adjusted R2	-0.018			-0.008			-0.017			-0.024		
Dependent Variable: SHAPS total score												
Constant	0.000	0.146	1.000	0.000	0.145	1.000	0.000	0.146	1.000	0.042	0.154	0.788
MRT	0.063	0.147	0.672				0.120	0.158	0.450	0.061	0.173	0.724
MF(AP)				0.017	0.146	0.429	0.160	0.158	0.316	0.211	0.170	0.219
MRT*MF(AP)										0.119	0.142	0.406
Adjusted R2	-0.018			-0.008			-0.017			-0.024		
Dependent Variable: PANAS negative affect												
Constant	0.000	0.137	1.000	0.000	0.146	1.000	0.000	0.138	1.000	0.014	0.147	0.925
MRT	**-0.343**	**0.139**	**0.017**				**-0.383**	**0.149**	**0.014**	-0.403	0.165	0.019
MF(AP)				0.003	0.147	0.866	-0.113	0.149	0.454	-0.095	0.161	0.558
MRT*MF(AP)										0.040	0.135	0.769
Adjusted R2	0.098			-0.021			0.090			0.071		

Table continues.

Table continued.

	Model 1 (M1)			Model 2 (M2)			Model 3 (M3)			Model 4 (M4)		
Variables	*B*	*SE*	*P*	*B*	*SE*	*P*	*B*	*SE*	*P*	*B*	*SE*	*P*
Dependent Variable: VAMS tension												
Constant	0.000	0.146	1.000	0.000	0.143	1.000	0.000	0.144	1.000	-0.070	0.151	0.647
MRT	-0.064	0.147	0.665				0.014	0.156	0.942	0.109	0.169	0.521
MF(AP)				0.206	0.144	0.160	0.210	0.156	0.185	0.125	0.166	0.455
MRT*MF(AP)										-0.198	0.138	0.159
Adjusted R2	-0.018			0.022			0.000			0.023		

Note. N=48. We examined the impact of mean reaction times (MRT) and mean frequency of approach decisions (MFAP) on depression severity as measured by BDI total score (top part) and anhedonia severity as measured by SHAPS total score (bottom part). *p values* smaller than 0.05 are in bold. All variables were z-scored before entering the regression.

Supplementary Table S7. *Sex differences in clinical scores and cognitive model parameters (based on the best-fitting model reported in the main manuscript).*

	females (n=35)		males (n=13)	
	M	*SD*	M	*SD*
Clinical scores				
Depression (BDI)	11.09	*9.78*	10.08	*8.86*
Anhedonia (SHAPS)	23.09	*5.96*	21.77	*6.76*
Positive Affect (PANAS)	27.46	*9.09*	33.62	*8.35*
Negative Affect (PANAS)	14.34	*6.10*	14.23	*3.68*
Tension (VAMS)	58.43	*23.06*	58.08	*23.83*
Sadness (VAMS)	29.89	*22.74*	22.38	*17.15*
Hostility (VAMS)	26.37	*22.60*	24.23	*20.19*
Cognitive model parameters				
Theta(conflict)	-0.03	*0.02*	-0.04	*0.01*
Theta(intercept)	0.55	*0.11*	0.55	*0.12*
Ter	0.63	*0.14*	0.65	*0.24*
zPBc	0.56	*0.07*	0.54	*0.06*
zPBi	0.00	*0.03*	0.00	*0.03*
a(conflict)	-0.04	*0.01*	-0.03	*0.01*
a(intercept)	1.85	*0.29*	1.94	*0.41*
v(averse):cD(positive)	0.25	*0.19*	0.26	*0.15*
v(averse)	-0.51	*0.18*	-0.62	*0.23*
v(reward):cD(positive)	-0.41	*0.02*	-0.40	*0.03*
v(reward)	0.60	*0.19*	0.62	*0.13*
v_cD(positive)	0.70	*0.58*	0.92	*0.50*
v(intercept)	0.51	*0.70*	0.39	*0.78*

Note. The description of the clinical scores can be found in the Method section and Supplementary Table S1. Moreover, the description of the parameters and their labels are introduced above (see also Supplementary Table S2 & S4). We do not provide any statistics on inference due to the large difference in sample size between females and males. This is merely a descriptive summary that serves for future research to study sex differences more systematically.

Supplementary Table S8. *Regression-based analyses associating symptom scores with best-fitting model parameters.*

Dependent Variable:	Θintercept	Θconflict	Ter	zPBc	zPBi	a_conflict	a_intercept
Positive Affect (PANAS)	-0.010	-0.049	-0.203	-0.051	0.011	0.172	-0.073
	(0.190)	(0.207)	(0.178)	(0.197)	(0.196)	(0.216)	(0.186)
Negative Affect (PANAS)	-0.542***	-0.195	-0.471**	-0.066	0.617***	0.047	-0.609***
	(0.187)	(0.204)	(0.175)	(0.194)	(0.193)	(0.212)	(0.183)
Sadness (VAMS)	-0.271	-0.264	-0.064	0.037	-0.173	0.284	-0.360*
	(0.215)	(0.234)	(0.200)	(0.222)	(0.221)	(0.243)	(0.210)
Tension (VAMS)	-0.263	0.274	-0.287*	-0.117	0.203	0.017	-0.226
	(0.175)	(0.191)	(0.163)	(0.181)	(0.180)	(0.198)	(0.171)
Hostility (VAMS)	0.018	0.209	-0.201	-0.063	-0.090	0.130	0.098
	(0.195)	(0.213)	(0.182)	(0.203)	(0.201)	(0.221)	(0.191)
Depression (BDI)	0.464**	-0.015	0.464**	-0.175	-0.001	0.010	0.386*
	(0.214)	(0.233)	(0.200)	(0.222)	(0.220)	(0.242)	(0.209)
Anhedonia (SHAPS)	0.043	0.140	0.147	-0.370**	-0.026	-0.152	-0.020
	(0.158)	(0.172)	(0.147)	(0.164)	(0.163)	(0.179)	(0.154)
BDI-by-SHAPS	0.069	0.091	0.104	0.056	-0.148	-0.068	0.075
	(0.130)	(0.142)	(0.122)	(0.135)	(0.134)	(0.148)	(0.128)
Constant	-0.035	-0.045	-0.052	-0.028	0.074	0.034	-0.038
	(0.148)	(0.162)	(0.138)	(0.154)	(0.153)	(0.168)	(0.145)
Observations	48	48	48	48	48	48	48
R^2	0.293	0.160	0.385	0.240	0.250	0.092	0.323
Adjusted R^2	0.148	-0.012	0.258	0.084	0.096	-0.094	0.185
Residual Std. Error	0.923 (df = 39)	1.006 (df = 39)	0.861 (df = 39)	0.957 (df = 39)	0.951 (df = 39)	1.046 (df = 39)	0.903 (df = 39)
F Statistic	2.023* (df = 8; 39)	0.931 (df = 8; 39)	3.047*** (df = 8; 39)	1.539 (df = 8; 39)	1.624 (df = 8; 39)	0.495 (df = 8; 39)	2.330** (df = 8; 39)
Note:	*p<0.1; **p<0.05; ***p<0.01						

Note. The description of the clinical scores can be found in the Method section and Supplementary Table S1. Moreover, the description of the parameters and their labels are introduced above (see also Supplementary Table S2 & S4).

Supplementary Table S9. *Regression-based analyses associating symptom scores with drift rates from best-fitting model.*

Dependent Variable:	Vintercept	Vreward	Vaverse	VcD(positive)	Vreward:cD(positive)	Vaverse:cD(positive)
Positive Affect (PANAS)	0.030	-0.235	0.099	0.192	-0.281	0.040
	(0.214)	(0.209)	(0.199)	(0.203)	(0.209)	(0.214)
Negative Affect (PANAS)	0.161	-0.149	-0.011	-0.307	0.097	0.216
	(0.211)	(0.206)	(0.196)	(0.200)	(0.206)	(0.211)
Sadness (VAMS)	-0.189	0.102	-0.063	0.436*	-0.098	-0.062
	(0.242)	(0.236)	(0.225)	(0.229)	(0.236)	(0.241)
Tension (VAMS)	0.165	-0.089	0.470**	-0.173	0.166	-0.178
	(0.197)	(0.192)	(0.183)	(0.187)	(0.192)	(0.197)
Hostility (VAMS)	0.045	0.038	0.376*	-0.069	-0.035	-0.244
	(0.220)	(0.215)	(0.205)	(0.208)	(0.215)	(0.220)
Depression (BDI)	0.260	0.041	0.239	-0.298	0.040	0.182
	(0.241)	(0.235)	(0.224)	(0.228)	(0.235)	(0.240)
Anhedonia (SHAPS)	-0.093	-0.001	-0.063	0.148	-0.237	0.066
	(0.178)	(0.173)	(0.166)	(0.168)	(0.174)	(0.177)
BDI-by-SHAPS	-0.148	0.104	-0.104	0.226	-0.135	-0.225
	(0.147)	(0.143)	(0.137)	(0.139)	(0.144)	(0.147)
Constant	0.074	-0.052	0.052	-0.114	0.068	0.113
	(0.167)	(0.163)	(0.156)	(0.158)	(0.163)	(0.167)
Observations	48	48	48	48	48	48
R^2	0.103	0.147	0.223	0.196	0.144	0.107
Adjusted R^2	-0.080	-0.028	0.064	0.031	-0.032	-0.076
Residual Std. Error	1.039 (df = 39)	1.014 (df = 39)	0.967 (df = 39)	0.984 (df = 39)	1.016 (df = 39)	1.037 (df = 39)
F Statistic	0.563 (df = 8; 39)	0.840 (df = 8; 39)	1.402 (df = 8; 39)	.188 (df = 8; 39)	0.820 (df = 8; 39)	0.585 (df = 8; 39)
Note:	*p<0.1; **p<0.05; ***p<0.01					

Note. The description of the clinical scores can be found in the Method section and Supplementary Table S1. Moreover, the description of the parameters and their labels are introduced above (see also Supplementary Table S2 & S4).

Supplementary Figures

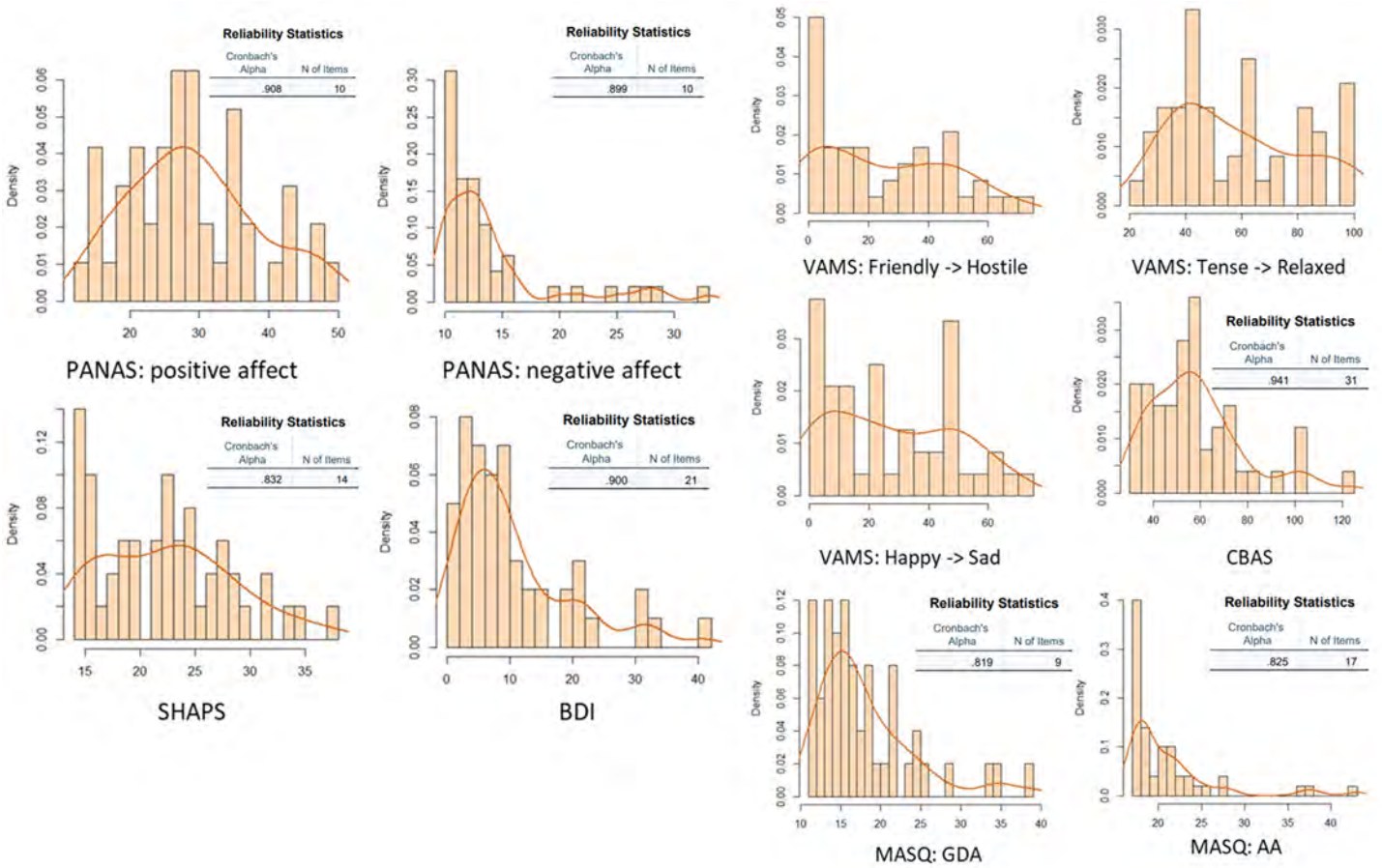

Supplementary Figure S1. Distribution and reliability measures across all clinical questionnaires. We refer to the Methods for a description of measures and interpretation of scores. Abbreviations: PANAS = Positive and Negative Affect Schedule; SHAPS = Snaith-Hamilton Pleasure Scale; BDI = Beck Depression Inventory; VAMS = Visual Analogue Mood Scale; CBAS = Cognitive and Behavioral Avoidance Scale; MASQ = Mood and Anxiety Symptom Questionnaire (GDA and AA are the anxiety-related subscores). All scales had excellent internal reliability (Cronbach's alpha ranging from 0.82 and 0.94. Note that since each VAMS score is a single item, measures of internal reliability are not needed.

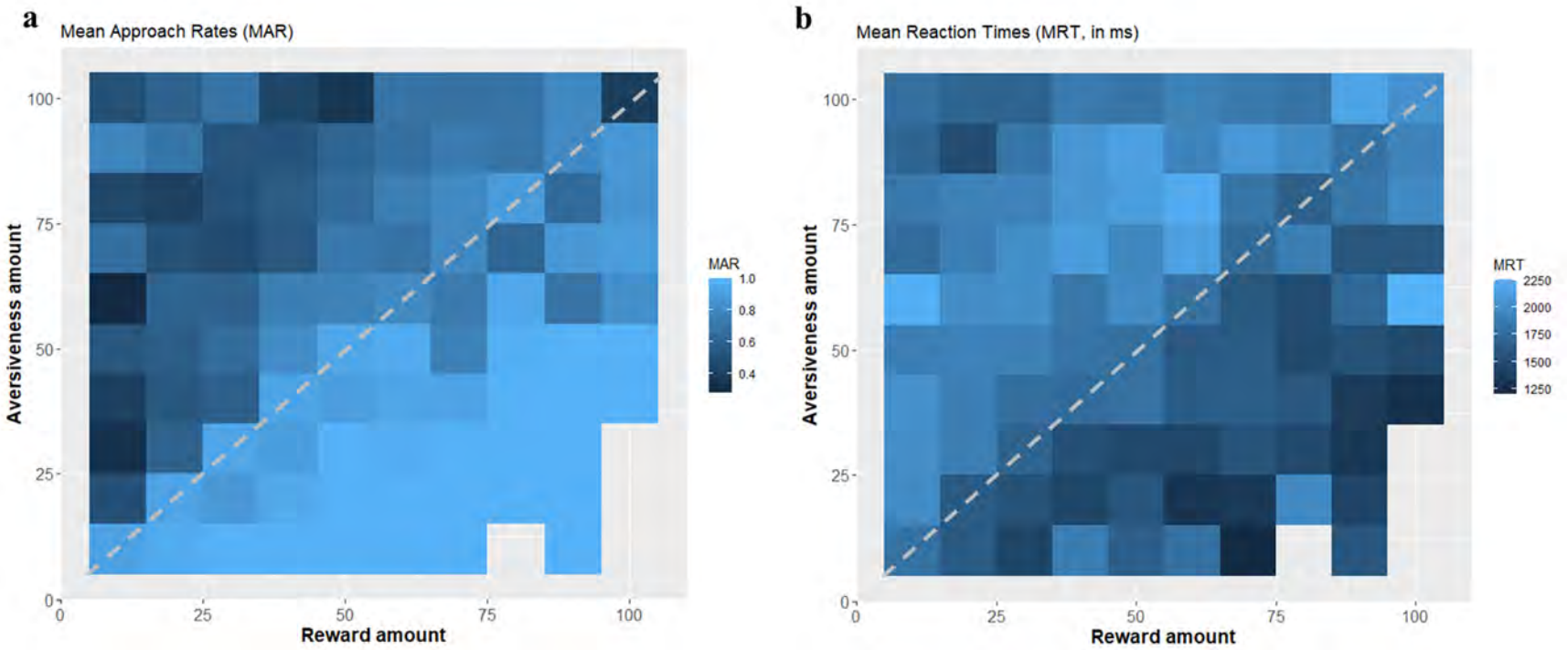

Supplementary Figure S2. a. Mean approach rates (MAR) for presented reward-aversiveness offers (aggregated across subjects). The grey-dotted line represents the forty-five-degree line, dividing the positive (below the grey line) and negative domains (above the grey line) based on offers' net values. b. Mean reaction times (MRT) for presented reward-aversiveness offers (aggregated across approach and avoidance decisions and across subjects).

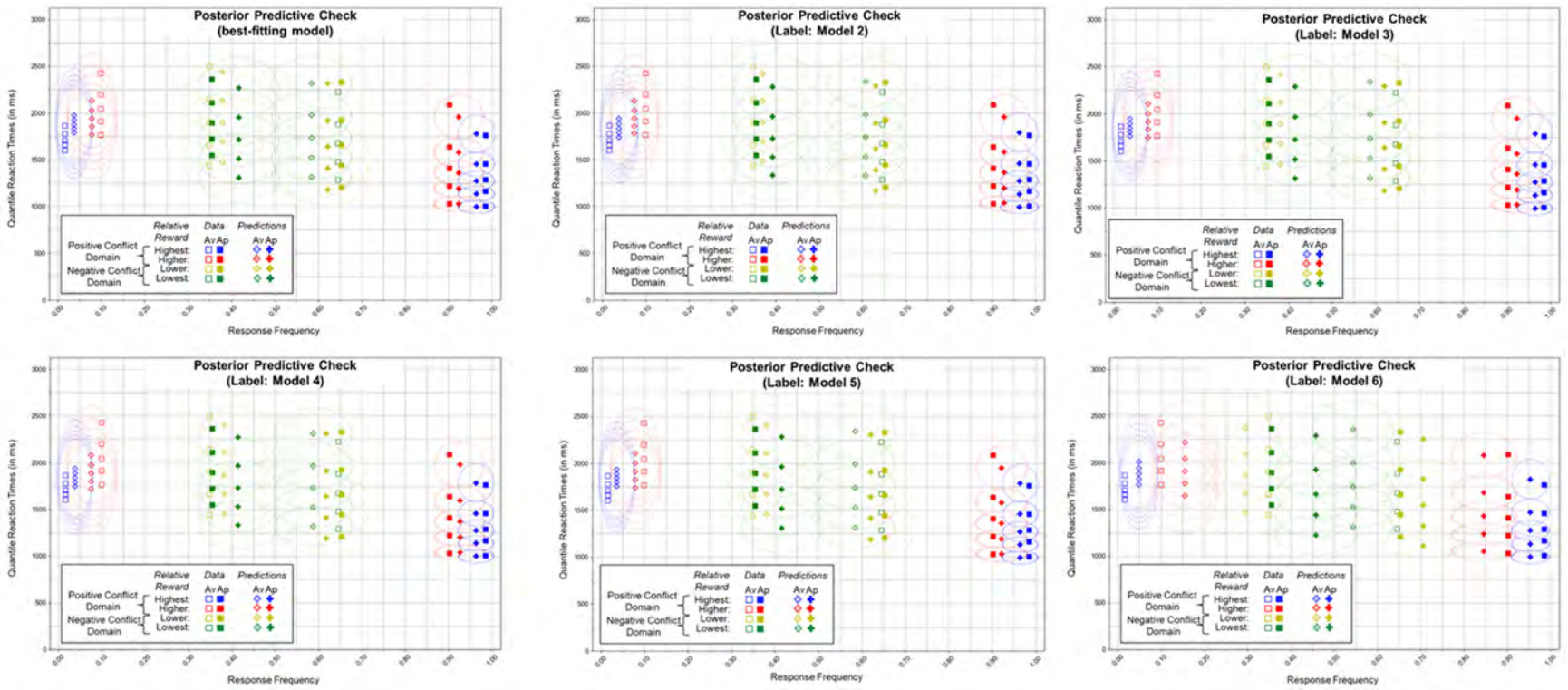

Supplementary Figure S3. Posterior Predictive Check of best-fitting model and selected models reported in the Supplementary Table s2 that show worse fits. For interpretation of quantile-probability plots, see main manuscript. Empirical behavioral choices and reaction time (RT) quantiles are represented as squares (unfilled for avoidance choices and filled for approach choices) and simulated choices and RTs from the posterior predictive check are represented as plus signs. RT quantiles are calculated for each subject separately and then averaged to obtain group quantiles. Ellipse widths (represented by dotted lines) index SD of the posterior predictive distribution from the model, indicating estimation uncertainty.

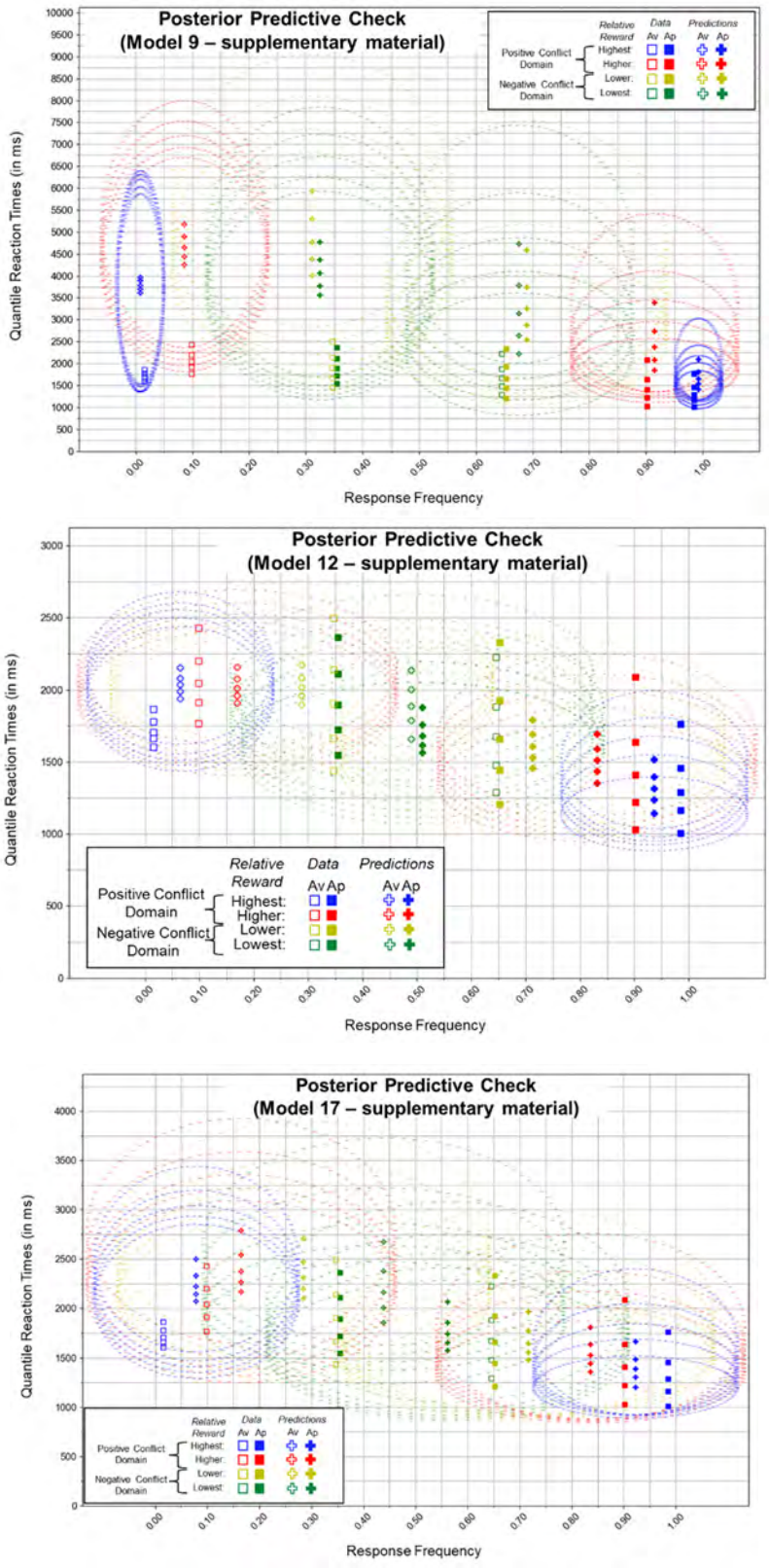

Supplementary Figure S4. Posterior Predictive Check of selected alternative models reported in Supplementary Table S2. For interpretation of quantile-probability plots, see main manuscript.

Empirical behavioral choices and reaction time (RT) quantiles are represented as squares (unfilled for avoidance choices and filled for approach choices) and simulated choices and RTs from the posterior predictive check are represented as plus signs. RT quantiles are calculated for each subject separately and then averaged to obtain group quantiles. Ellipse widths (represented by dotted lines) index SD of the posterior predictive distribution from the model, indicating estimation uncertainty.

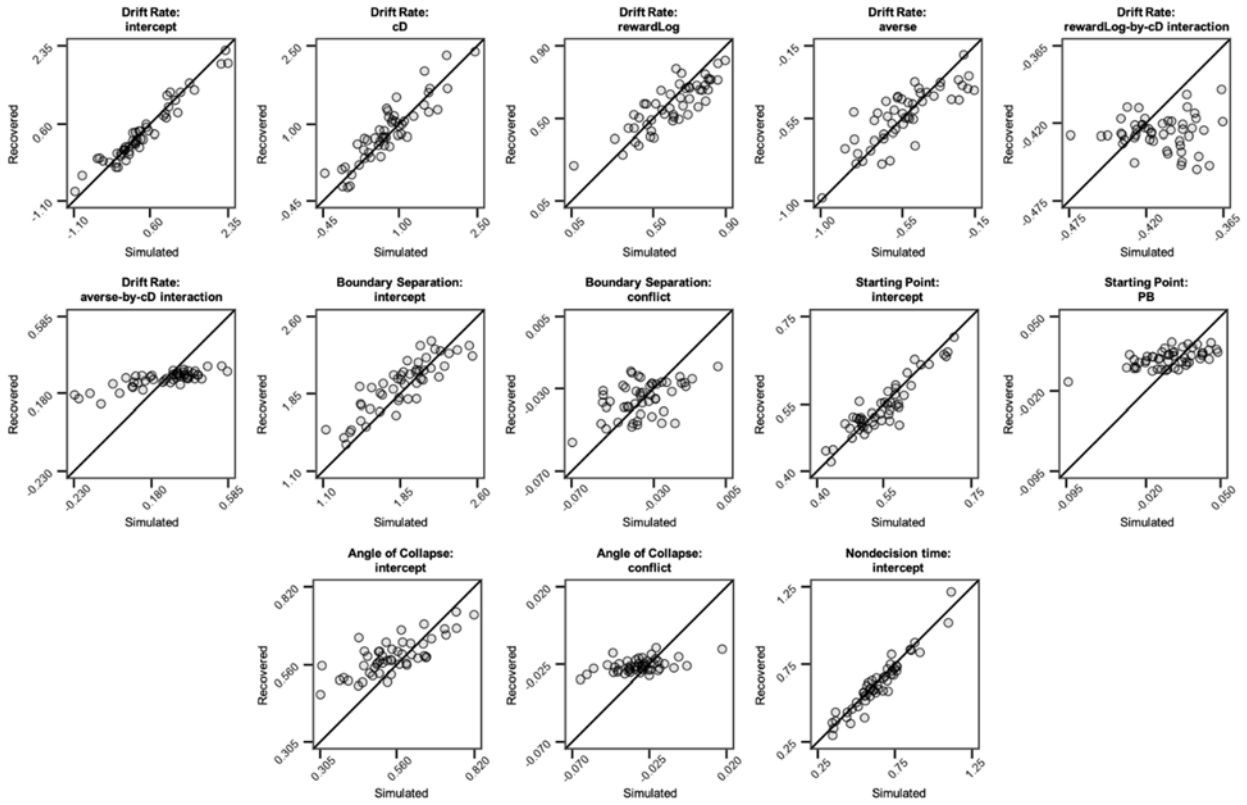

Supplementary Figure S5. Results from simulations comparing input parameters (x-axis) and recovered parameters (y-axis). Overall, these plots show good parameter recovery with better recovery for parameters in the negative than the positive domain.

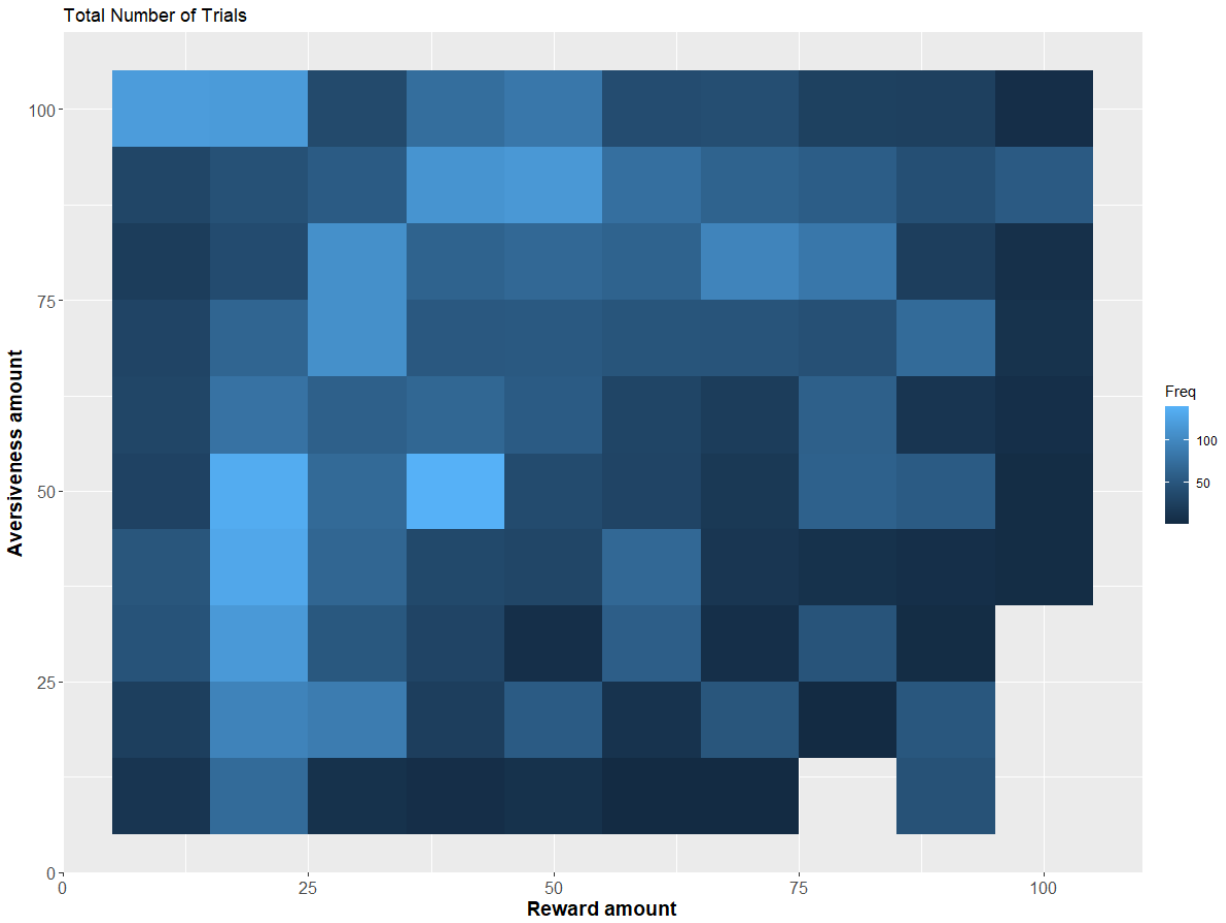

Supplementary Figure S6. Number of trials for presented reward-aversion offer (averaged across all participants).

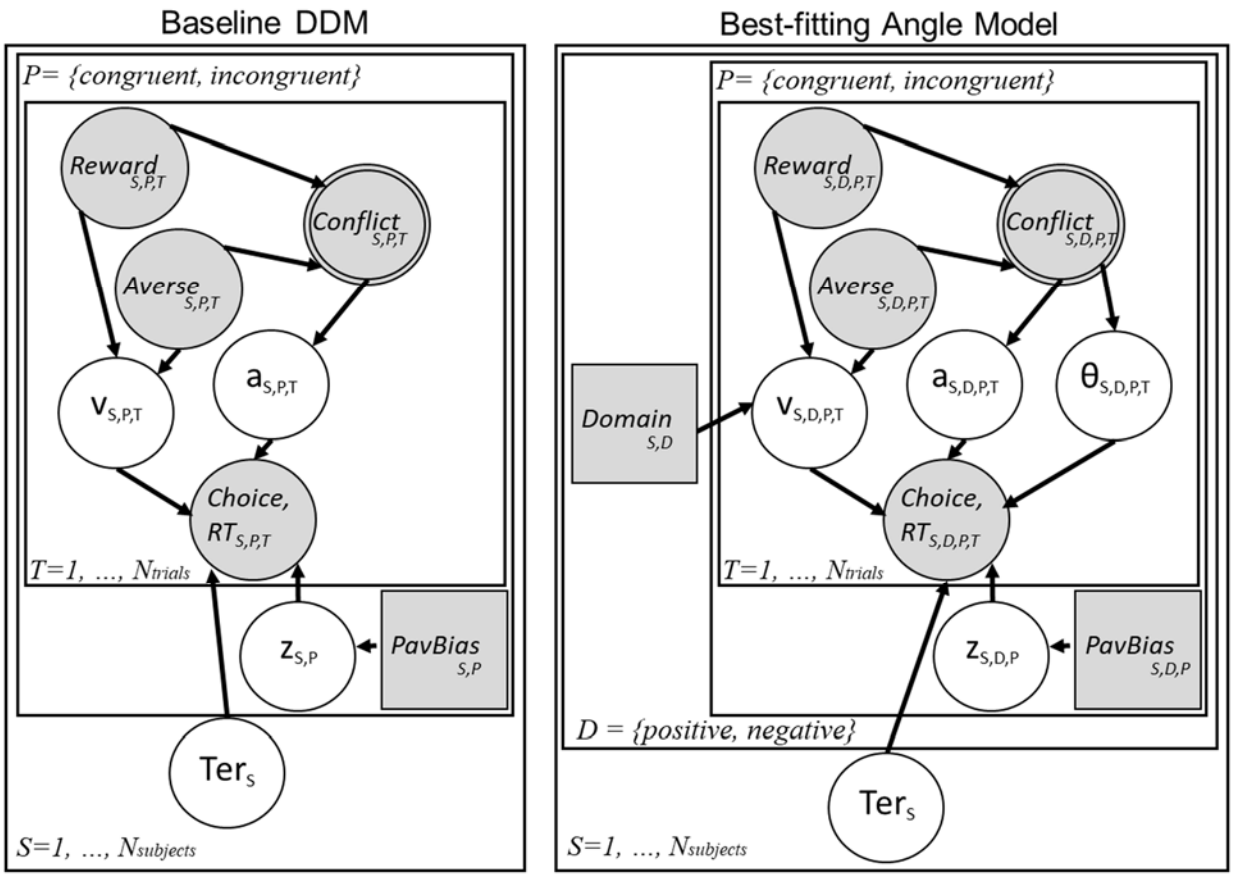

Supplementary Figure S7. Graphical representation of the DDM specification (left) introduced by Pedersen et al. (2021) and used as the baseline model (see Methods); and the best-fitting Angle model (right). Shaded nodes represent observed variables, non-shaded nodes represent estimated parameters (a=boundary separation, z=starting points, v=drift rate, Ter=nondecision time, θ=angle of linear collapse). Circles represent continuous variables; squares represent discrete variables. Conflict refers to the absolute difference between reward and aversion and is therefore computed and double-bordered. Variable subscripts: S=subjects, D=domain, P=Pavlovian-congruency, T=trials.

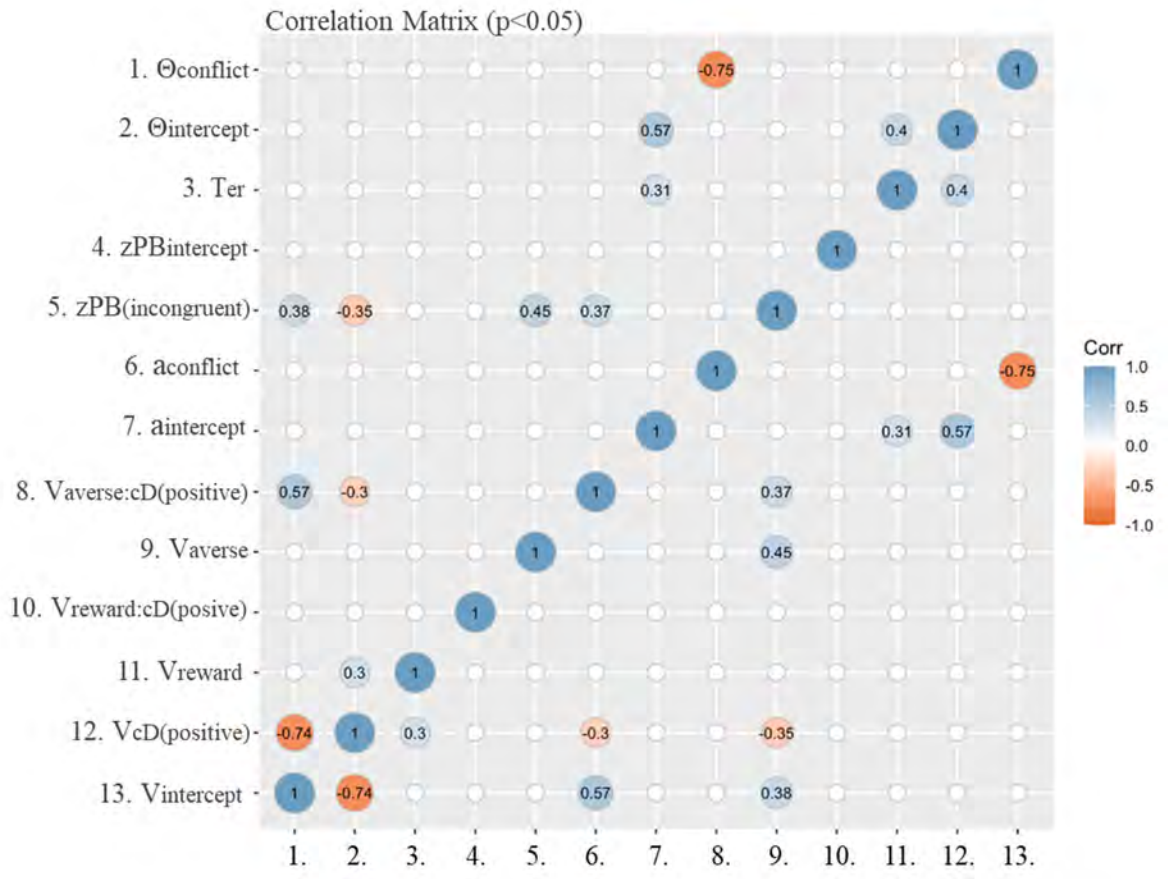

Supplementary Figure S8. Relationship between parameters of the best-fitting model discussed in the main manuscript. Only significant correlations (Corr) are shown. The parameter labels (along the y-axis) correspond to the same parameter labels in the Supplementary Table S4 which shows the posterior statistics of each parameter (i.e., θ=angle of boundary collapse, Ter=nondecision time component, zPB=starting point bias as a function of Pavlovian-congruent response mapping, a=boundary separation, v=drift rates). The number labels along the x-axis correspond to the same numbers along the y-axis.

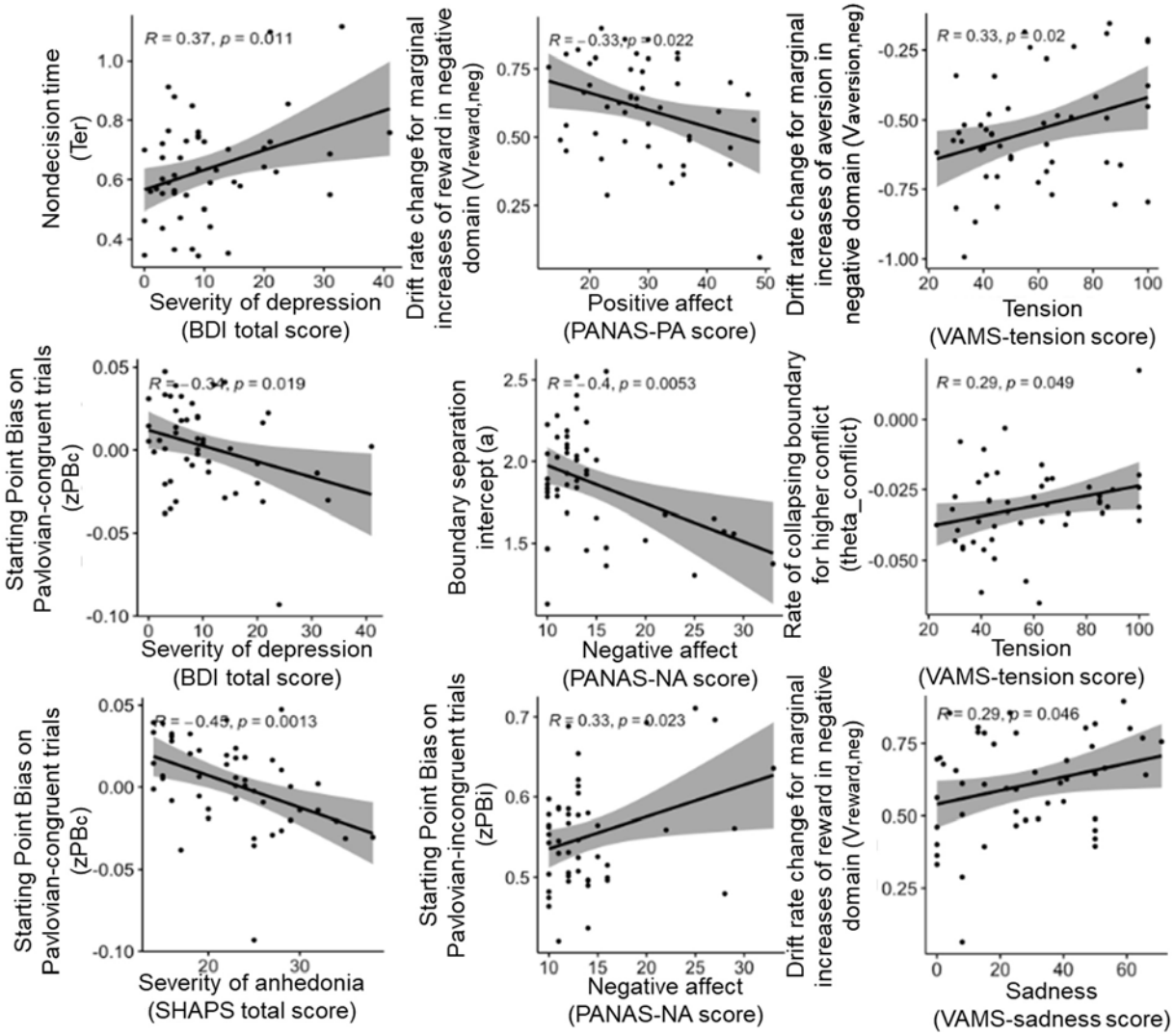

Supplementary Figure S9. Scatterplots of all significant associations shown in Figure 3 of the main manuscript. Black dots indicate data. Shown are means (solid lines) and corresponding 95% confidence intervals as shaded intervals (R=correlation coefficient; p=p-value).

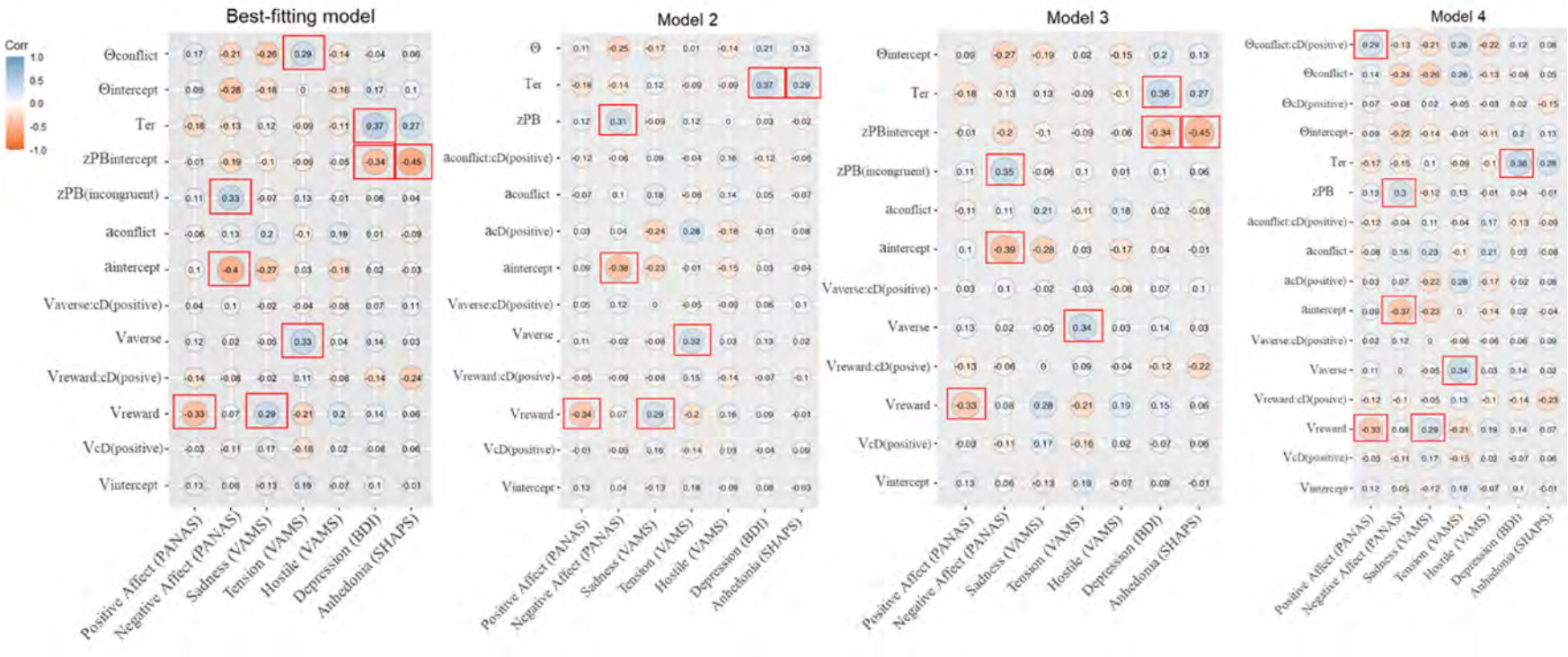

Supplementary Figure S10. Relationship between model parameters (of the best-fitting model discussed in the main manuscript) and clinical scores. The first correlation matrix from left shows associations for the best-fitting model discussed in the main manuscript (see also Supplementary Table S4 which shows the posterior statistics of each parameter). The other four correlation matrices show association for the three next models based on posterior predictive checks shown in Supplementary Figure S2. The model labels correspond to those introduced in Supplementary Table S2. The significant (p-values < 0.05 and unadjusted for multiple comparisons) are surrounded by red boxes.